Diplomarbeit

Electrical Stimulation of the Spinal Cord to Decrease Pain

Elektrostimulation der Wirbelsäule zur Verringerung von Schmerzen

unter der Anleitung von

Ao.Univ.Prof.i.R. Privatdoz. Dipl.-Ing. Dr.sc.med. Dr.techn. Dr.rer.nat.

Frank Rattay

Institut für Analysis und Scientific Computing

Technische Universität Wien

Studentin

Pegah Tafvizi

Wien, October 2020

I confirm that this work is original and has not been submitted elsewhere for any examination, nor is it currently under consideration for a thesis elsewhere.

Vienna, August 2020

Acknowledgments

I also want to thank God, thanks to my father, my mother, and my husband; without you, I would not be able to be where I am now.

I would also like to thank the dean of studies, professor Eugenijus Kaniusas, and my thesis adviser Professor Frank Rattay for their guidance, help, and constant support during my master study and the research work.

Table of Contents

Abstract

Pain is a global health issue that can prevent a human being from doing their essential daily tasks and is significant suffering for anybody who has it. Conventionally, drugs and medication have been used to decrease or relieve pain. However, with increased technological advancements in the medical field, electrical neural stimulation has been adopted, especially in first world countries. This emerging technology has been proven to be very helpful. One of the FDA approvals for electrical neural stimulation technology is the Electrical Stimulation of the Spinal Cord (SCS to reduce human pain.

The mechanisms of SCS and other factors influencing SCS are explained in this thesis. The three waveforms which are currently used clinically for SCS are (i) conventional/tonic SCS (typically in the range of 20-120Hz), (ii) burst SCS (five consecutive 500Hz waves at 40Hz burst frequency), and (iii) high-frequency SCS (HF10 SCS is 10kHz frequency). Several studies have shown that high-frequency SCS and burst SCS do not cause paresthesia and are the most effective waveforms for pain SCS. In chapter 6, I used the Hodgkin Huxley for a single-compartment neuron model in MATLAB. I modeled the three SCS waveforms using MATLAB and checked the effects of these waveform stimulations separately in the single-compartment neuron model. For future study, one good idea is to check the impact of a new pattern of the waveform on a single neuron model or multi-compartment neuron model or check the effect using the voltage-clamp technique in a laboratory. Brain images could also be used in this recommendation for future study as well as to observe different waveform pattern effects and find the most pain relief waveform pattern for SCS.

It is hoped that this thesis study would give a good overview of SCS and provide helpful hints to other fellow researchers as well as general medical healthcare personnel in various ways to improve the technology.

Deutsche Kurzfassung

Schmerz ist ein weltweites Gesundheitsproblem, welcher Menschen von deren täglichen Aufgaben abhält und großes Leiden für die Betroffenen bedeutet. Die konventionelle Behandlungsmethode ist der Einsatz von Medikamenten, welche die Schmerzen lindern oder die Patientinnen und Patienten gänzlich davon befreien. Die Entwicklung neuer Technologien im medizinischen Bereich, vor allem in Erste Welt-Ländern, macht es möglich, elektrische Nervenstimulation zur Schmerzlinderung anzuwenden. Diese neu entstandene Technologie hat sich als sehr verheißungsvoll erwiesen. Eine der FDA Zulassungen für elektrische Nervenstimulation ist die Rückenmarkstimulation (SCS) zur Linderung menschlichen Schmerzes.

In dieser Arbeit wird der Mechanismus von SCS erklärt und Faktoren, die SCS beeinflussen, aufgeführt. In der klinischen Anwendung werden drei Stimulationsformen von SCS eingesetzt: (i) konventionelle/niedrigfrequente SCS (im Bereich von 20-120 Hz), (ii) burst SCS (fünf aufeinander folgende Impulse von jeweils 500 Hz, 40 mal pro Sekunde) und (iii) hochfrequente SCS (10 kHz). Mehrere Studien haben gezeigt, dass die hochfrequente SCS als auch die burst SCS keine Parästhesie verursachen und sich als die effizientesten Formen der Schmerzbehandlung bewähren.

In Kapitel 6 habe ich das Hodgkin Huxley-Modell angewandt, um ein Ein-Kompartiment-Modell einer Nervenzelle in MATLAB zu implementieren. Ich habe die drei Stimulationsmöglichkeiten von SCS in MATLAB simuliert und die Effekte der drei Stimulationen an der Nervenzelle im Modell verglichen.

In weiteren Untersuchungen konnte der Einfluss von neuen Mustern der Stimulation auf das Ein-Kompartiment-Modell oder auf ein Multi-Kompartiment-Modell berechnet werden. Weiters konnte der Einsatz der Voltage-Clamp Technik im Labor untersucht werden. Auch Bildgebungsverfahren des menschlichen Gehirns könnten in zukünftigen Studien eingesetzt werden, um die Effekte verschiedener Stimulationsmuster zu untersuchen und eine Variante zu finden, die den besten Erfolg zur Schmerzlinderung führt.

Diese Arbeit soll einen Überblick über SCS ermöglichen und hilfreiche Hinweise für zukünftige Forschungsarbeiten und medizinisches Personal bieten, um die Technologie weiterhin zu verbessern.

List of Abbreviation and Symbols

ADA	Anno Domini (since the time of Christ)
ANS	Advanced Neuromodulation Systems
AP	Action Potential
ATP	Adenosine Triphosphate
BC	Before Christ (before the birth of Jesus)
CNS	Central Nervous System
CRPS	Complex Regional Pain Syndrome
CT scan	Computed Tomography scan
ETSEMG	Triggered Stimulation
FBSS	Failed Back Surgery Syndrome
FDA	Food and Drug Administration
FES	Functional Electrical Stimulation
GABA	γ-aminobutyric acid
IFC	Interferential current
IPG	Impulse generator
MRI	Magnetic resonance imaging
NGF	Nerve Growth Factor

NMES	Neuromuscular electrical stimulation
PNS	Peripheral Nervous System
RETS	Reciprocal EMG Triggered Stimulation
SCS	Stimulation of Spinal Cord
TENS	Electric Nerve Stimulation
TPRA1	Transient receptor potential ankyrin 1
TRP	Transient receptor potential
TRPM8	Transient receptor potential cation channel subfamily M member 8
TRPV1	The transient receptor potential cation channel subfamily V member 1
TTX	Tetrodotoxin
TTX-R	Tetrodoxin Resistance
VNS	Vagus Nerve Stimulation

Glossary:

Action Potential…….	A rapid change of membrane potential (e.g.eg, from resting membrane potential (-70 millivolts to a rising voltage of +40 millivolts (for depolarization state)).
Cessation of smoking……..	Quitting smoking
Cm…….	The membrane capacity
Dermatome……	Is an area of skin with sensory nerves of a single spinal nerve root.
Excitatory agents……..	Promote generating an action potential
Exogenous chemicals……	Chemical from outside of the body
F……	Faraday Constant which is 96485 [C /mole]
GABA……..…….	Inhibitory neurotransmitter

Glutamate……	Excitatory neurotransmitter
HF10 SCS……..	Stimulation of Spinal Cord with 10kHz frequency
Inhibitory agents……	Prevent generating an action potential
I_m……..……..	Membrane current
I_{Na}, I_k, I_L ……	Membrane current for (sodium, potassium, leakage)
i_{st} ……	Stimulating Current Density in [$\mu A/cm^2$]
i_i…….	Ionic Current Density in [$\mu A/cm^2$]
i_{Na}, i_K, i_L, i_P……..	Sodium, Potassium, Leakage and Nonspecific Current Densities in [$\mu A/cm^2$]
Ligand-gated ion channel……..…	Is a membrane protein that gets open when the ligand bonds to the receptor and gets close after leaving the receptor.
Ligand……..……..	A molecule which binds to the receptor.
Myocyte……...	Muscle cell
Percutaneous…….……....	Penetrating through the skin by a needle (no open surgery)

Projection neuron…….	These are neural cells in the CNS whose axons extent to several other parts of the CNS
P_{Na}……	Sodium Permeability Constant which is 0.008[cm /s]
P_k……..	Potassium Permeability which is 0.0012 [cm / s]
P_p……..	Nonspecific Permeability which is 0.00054 [cm / s]
R……..	Gas Constant which is 8314.4 [mJ / K/ mole]
T…….	Absolute Temperature which is 293.15 [0 .K) (=20°C)
Somatosensory…….……	Relates to sensation (such as itch, touch, pain, temperature, pressure), which feel it like the whole body feels it and not only one specific organ like the eye can sense it.
Sub sensory ……..……...	Below the threshold of sensation or consciousness
V_{rest}…….	Resting Potential defined as -65 [mV] here

V_L … … … … … … … … … … . … … … … … ….	Leakage Voltage which is 0.026 [mV]
Wide-Dynamic Range neuron……..	Are neurons in the spinal cord that receive A-beta, A-delta and C fibers information. Wide-Dynamic range neuron responds to non-painful stimuli and painful stimuli.

1. Pain

1.1 Introduction

The word pain originates the Latin word ‘Poena’ which literarily translates to punishment.

Pain is described as unpleasant emotional experiences linked to real or potential harm. When we cut our finger and feel pain, the pain happens in four steps: transduction, transmission, modulation, and perception. Transduction and transmission occur in the peripheral nervous system (PNS), whereas modulation and perception occur in the central nervous system (CNS):

(i) Transduction is the process whereby the nociceptors are activated because of the injured tissue.

(ii) Transmission is the process of sending information from the nociceptors to the central nervous system.

(iii) Modulation is the passing of information in the spinal cord's dorsal horn, where the first-order neuron synapses to the second-order neuron.

(iv) Perception is the process of explaining the signal, which causes an emotional response perceived by the brain (see Figure 1.1).

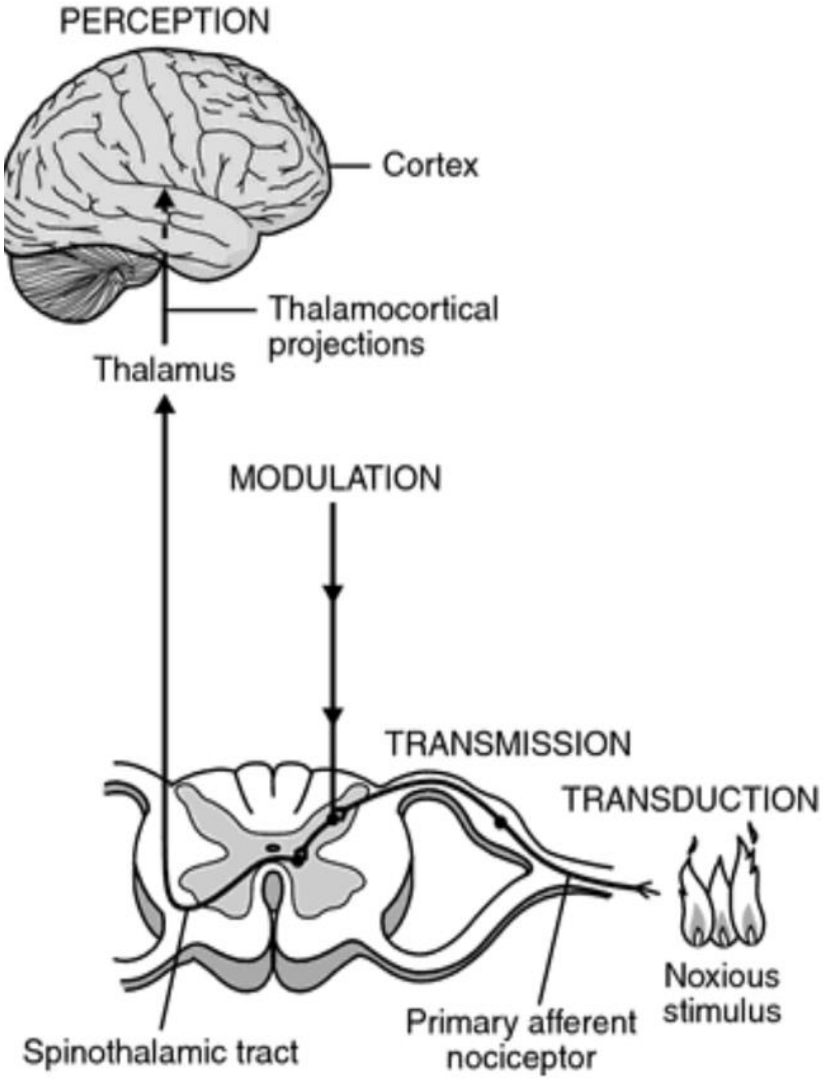

Figure 1.1 The four steps of transduction, transmission, modulation, and perception.

1.2 Nociceptors

The word "nociceptor" is derived from the Latin term "nocer" meaning "to harm or damage". A nociceptor is a neuronal receptor of mechanical, thermal, and chemical injurious stimulant and is an essential unit of the transduction step of the pain process (see Figure 1. 2)

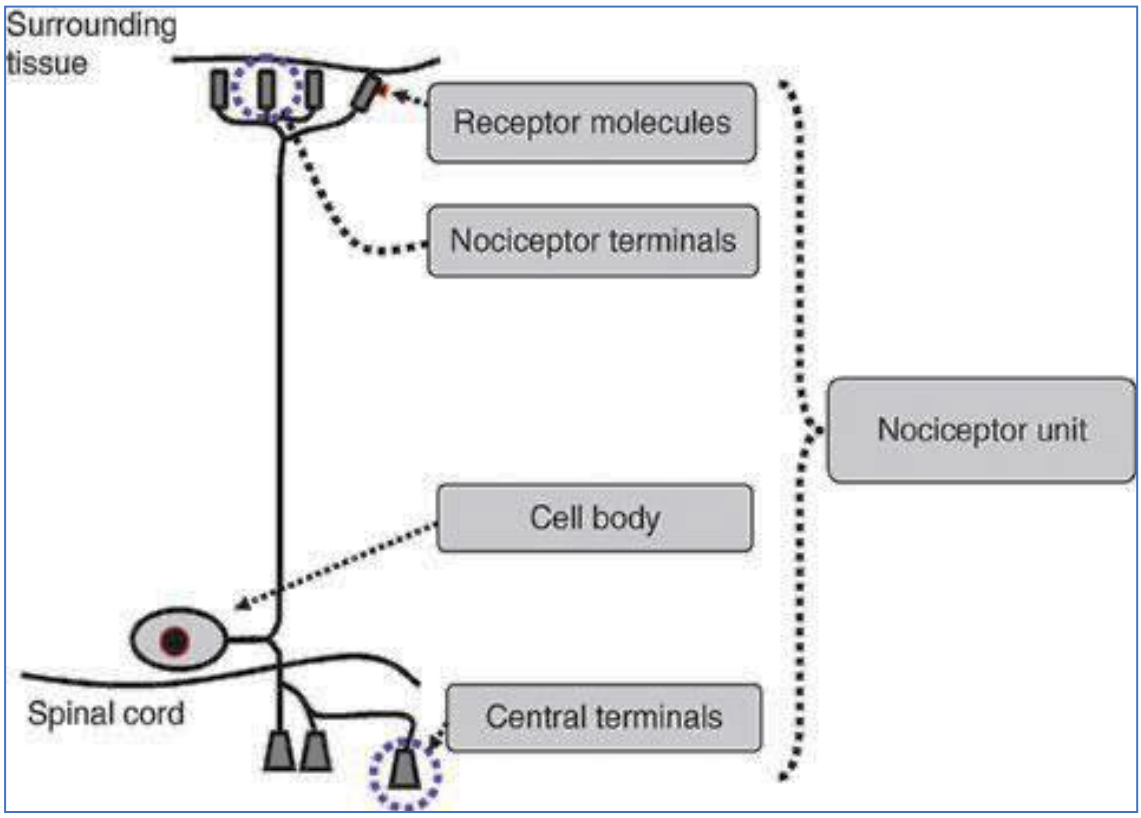

Figure 1.1 Schematic diagram of the relevant parts of a nociceptive neuron.

The pain signal is transmitted by action potentials traveling down to neuronal axons mainly caused by the entrance of sodium ions (the voltage-gated channel influx) at a certain threshold. There are two types of sodium channels on nociceptors that play a role in pain production. The first is called tetrodotoxin-resistant (TTX-R). The second is called

tetrodotoxin sensitive (TTX-S, which needs lower action potential thresholds than TTX-R).

Ligand-gated ion channel interacts with the receptor, which leads to a conformational change that results in opening or closing the membrane ions channel. Opening or closing the ion channels causes ions such as Na+, K+, Ca2+, and Cl− pass through the membrane and results in a potential change of cell membrane. Therefore, excitatory receptor activation can result in depolarization, whereas an inhibitory receptor activation can result in hyperpolarization (Cohen and Mao 2014, Bonica 2010).

For example, transient receptor potential ankyrin 1 (TRPA1) is an ion channel sensitive to temperature and chemical stimuli (Laursen 2015). When something icy is touched, TRPA1 responds to the noxious cold. It allows mainly sodium and calcium influx into the nerve terminal, causing an action potential to generate (Figure 1.3). In essence, when the nociceptor threshold is reached, they convert the initial stimulus into electrical activity. If membrane potential goes to about -55mV, the neuron will have an action potential. TRPA1 is found on the peripheral terminals as well as in central terminals of primary afferent primary nerve fibers (Koivisto, 2014). TRPA1 amplifies the glutamate release at the dorsal horn of the spinal cord, which further depolarizes the second order neuron of the spinal cord (Castro-Junior et al. 2018).

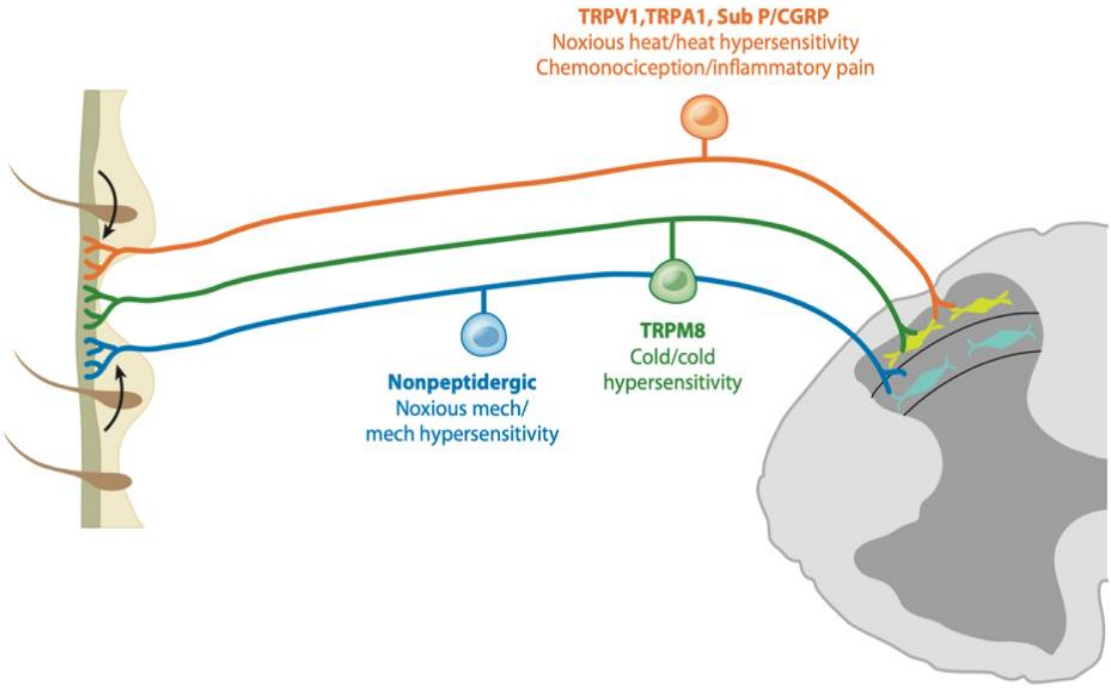

Figure 1.3 Transient receptor potential (TRP) channels. (TRP) are activated by specific factors, such as hot or cold stimuli. TRPV1- (orange) nociceptors mediate sensitivity to noxious heat; TRPM8 (green) neurons mediate sensitivity to cold (Julius 2013).

On the other hand, when nociceptors are activated, they release various chemical mediators from their peripheral terminals, like substance P. The chemical mediators remain even after the initial physical stimulus has passed. These chemical mediators sometimes can cause pain to persist beyond the duration of the initial noxious stimulation (Davis et al. 2020).

Chemical mediators of inflammation also sensitize nociceptors, reducing their activation threshold to their stimuli (Beck and Handwerker 1974, Berberich et al. 1988). This process is known as peripheral sensation.

1.3 Types of pain

We can divide pain into three categories (i) nociceptive pain, (ii) neuropathic pain, (iii) inflammatory pain:

(i) Nociceptive pain (acute pain) is the result of the pain-processing steps explained in Figure 1.1. This pain helps our hand pull away from a hot oven, allowing us to escape by a fast reaction to danger.

(ii) Neuropathic pain is described as pain resulting from nerve damage or the nerve's altered function. There are also many other definitions for neuropathic pain; one widely accepted explanation for neuropathic pain is a pain caused by the somatosensory system disease, including peripheral fibers (A-beta, A-delta, and C fibers) and central neurons. Neuropathic pain affects 7–10% of the general population (Colloca et al. 2017).

(iii) Inflammatory pain is associated with tissue damage and inflammation. Inflammatory pain, unlike acute pain, is like an alarm for reminding a recent injury. It discourages us from doing activities with the injured area. Inflammation can be either

i. **Inflammatory acute pain** is short-lived, and it goes away within hours or days.
ii. **Inflammatory chronic pain** is long-lasting, and it stays for months or even years, even after the first trigger is gone (see Figure 1.4).

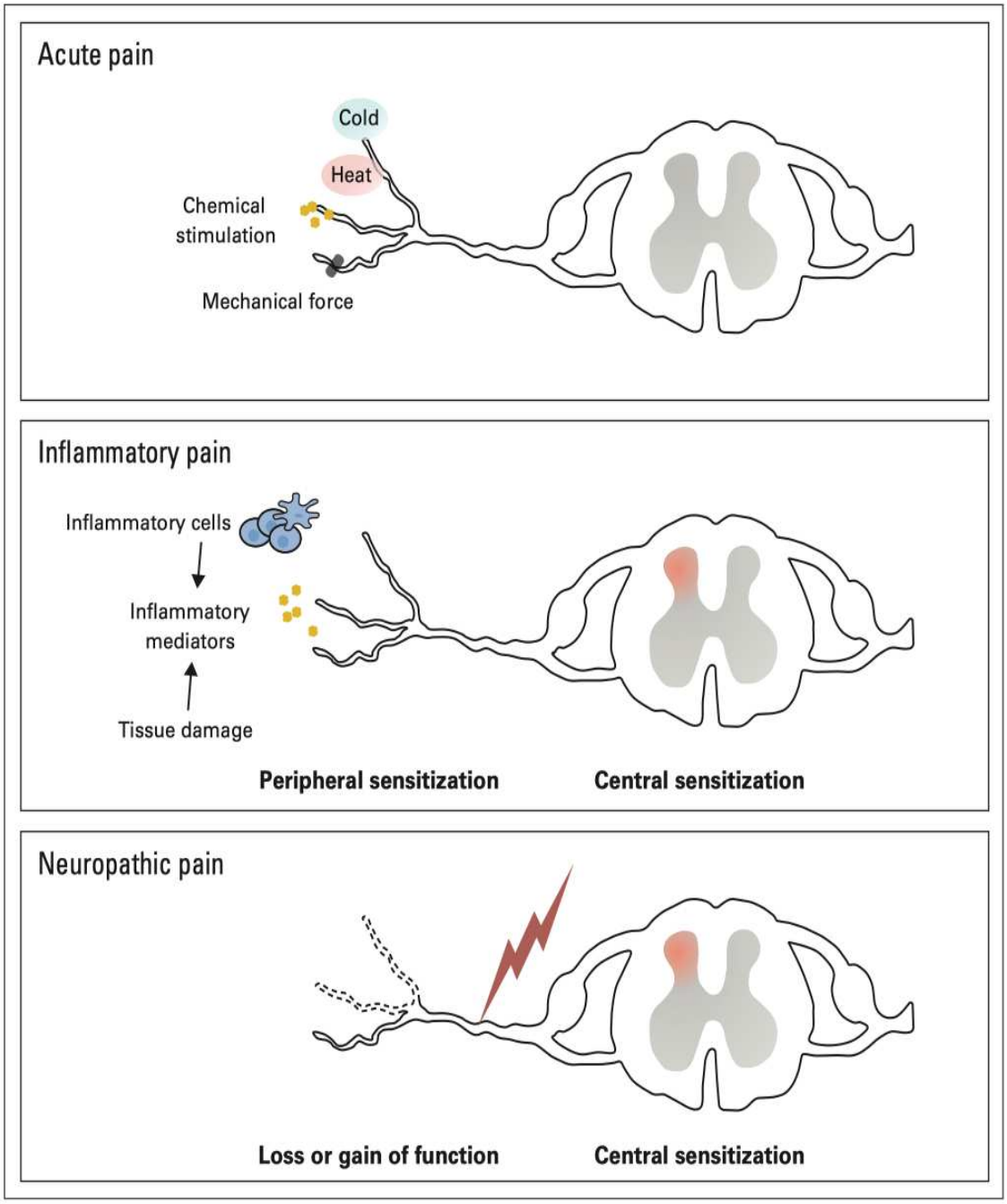

Figure 1.4 Different types of pain.

1.4 Nerve fibers

Nociceptors are the terminals of two types of primary afferent neurons: C-fibers and A-delta fibers. C-fibers nerves are the shortest in diameter and are unmyelinated, transmitting their electric signal at a speed of 1.0-4.0 meter/second (Elliott 1994). They transmit sensations like burning or aching (Ochoa and Torebjork 1983, Torebjork and Ochoa 1984). Pain sensations transmitted by C fibers are long-lasting and have autonomic responses such as increased heart rate and blood pressure.

Below, there is a small summary of the four different nerve fibers

- A-alpha nerve fibers relay signals related to kinesthesia.
- A-beta nerve fibers relay signals related to touch.
- A-delta nerve fibers relay signals related to pain and temperature.
- C-nerve fibers transmit pain, temperature and itching information.

The fiber diameter is an essential variable for the stimulation of the spinal cord. The dorsal column in the human spinal cord is composed of axons with various diameters (average diameter ~ 5.0 Micrometer and a maximum diameter of 16.0 Micrometer at lower thoracic levels for the myelinated axons) (Feirabend et al. 2002). (Figure 1.5) shows the diameter and velocity of the four nerve fiber types. The length of an axon, however, is highly variable, depending on its location.

The voltage-gated channel lies along the entire length of the membrane of the unmyelinated axons. In comparison, the voltage-gated channel in myelinated axons is only in the nodes of the Ranvier. The action potential in the myelinated axon is amplified in every internode of Ranvier (Rattay 1986). Therefore, the unmyelinated axons have a lower conduction speed of the nerve signal (action potential). In the myelinated fibers, the large-diameter fibers have a lower threshold current for extracellular stimulation than smaller fibers (Struijk 1992).

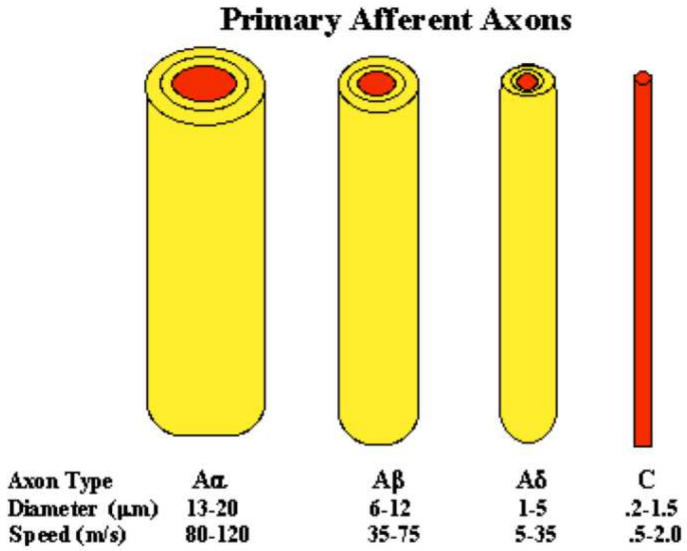

Figure 1.5 Fiber diameter and speed of passing signal in A-alpha, A-beta, A-delta, and C-nerve. The higher the diameter of a nerve fiber (thicker myelinated fiber), the faster the speed of passing the action potential.

1.5 Different treatments for pain

Many European doctors gave opium to their patients in the 1600's to alleviate pain. In 1806 Serturner described the active ingredient of opium and named it morphine after Morpheus, the God of dreams. Morphine constitutes 12% of opium.

Codeine was also used to alleviate pain soon afterward (Brownstein, 1993). In 1873 Charles von Gerhardt prepared a more appropriate version of the drug with the addition of an acetyl ring, synthesizing what is widely called aspirin today (Fairley 1978). Soon after that, Bayer licensed aspirin and commercialized it in 1899. Some types of drugs which are still in use today are taking their root from ancient traditional medicines.

In addition, British surgeon James Moore showed early in 1784 that specific compression of the nerves could react to reversible operative anesthesia and, thus, regional nerve blockade (Moore 1784). In 1936, at Bellevue Hospital in New York City, the first pain management using a nerve block technique was established (Rovenstine 1941).

Explaining how electricity induced pain relief was not clarified until gate control theory became a part of the understanding of the pain specialist (Sabatowski et al. 1992).

With the aid of the gate control theory and other explanations, there are many non-drug pain management like electrical stimulators of the spinal cord (SCS), transcutaneous electric nerve stimulation (TENS) units, deep brain stimulation, light therapy, intra-articular ozone therapy, hypnosis, etc.

To determine which pain medication is better suited for a patient, doctors must evaluate the location, intensity, and type of pain pathophysiology. They are filled out based on the patient's history, pain questionnaire, and physical examination (Grond et al. 1996).

2. Stimulation

2.1 Types, uses, and examples

There are several kinds of electrical stimulation used for different treatments. Example of using stimulation for treating human are,

- Deep brain stimulation to treat depression
- **Functional electrical stimulation (FES)** uses trains of electrical stimulation to induce body movements in individuals with central nervous system injuries
- Spinal cord stimulation to decrease pain
- **Vagus nerve stimulation (VNS)** for treating depression or pain
- **Neuromuscular electrical stimulation (NMES)** to help muscle movement. NMES uses electrical impulses that directly stimulate motor neurons. The terms **FES (Functional Electrical Stimulation)**, **ETS (EMG Triggered Stimulation)**,

and **RETS (Reciprocal EMG Triggered Stimulation)** fall under the NMES category as well.

- **Transcutaneous electrical nerve stimulation (TENS)** is used in symptomatic relief of chronic pain or temporary release of constant muscle pain.
- **Interferential current stimulation (IFC)** to decrease pain.

2.2 Comparison of the Hodgkin-Huxley and the Frankenhaeyser-Huxley model

2.2.1 Hodgkin-Huxley model

In 1952, Alan Hodgkin and Andrew Huxley described the mathematical model for propagating action potentials in large diameter axons of squid. The model consists of four nonlinear differential equations approximating the electrical properties of excitable cells like neurons. The equivalent electrical circuit of the Hodgkin-Huxley nerve membrane model is shown in Figure 2.1. the voltage-clamp technique used also shows in Figure 2.2. The action potential propagation is related to the nerve's excitation and not to the synapses that depend on the concentration of neurotransmitters and a few other parameters. Therefore we can exclude the influence of neurotransmitters and other chemical effects in the Hodgkin-Huxley equation.

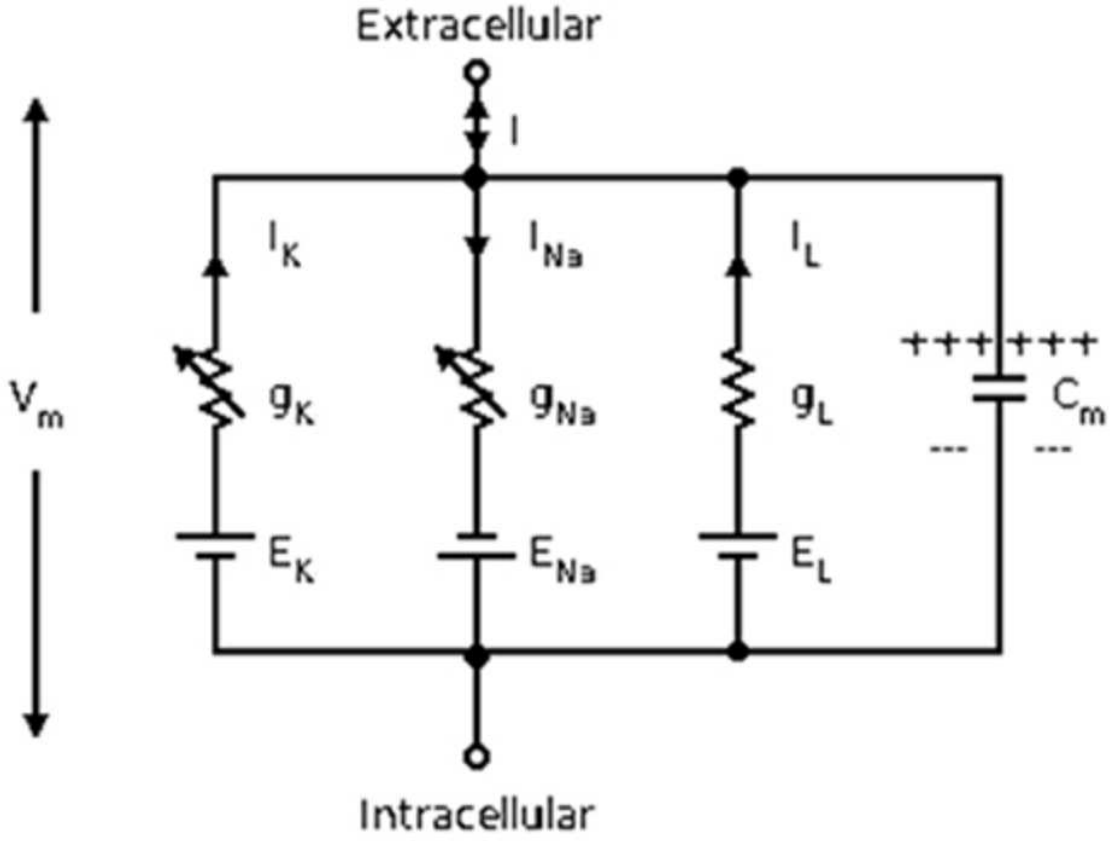

Figure 2.1 The cell membrane electrical circuit model for the Hodgkin-Huxley model. The Cm is the membrane capacity. The g's represent the conductance of the ions types. Ionic membrane is the sum of the I(k) potassium current, the I(Na) sodium current and the I(L) small leakage current due to other ions. Each ions current is calculated as the voltage drop across that conductor multiply by the gating force (G). G is defined as 1/g. Therefore we have :

$$I_m = C_m \frac{\partial V}{\partial t} + G_{Na}(V_m - V_{Na}) + G_k(V_m - V_k) + G_L(V_m - V_L)$$

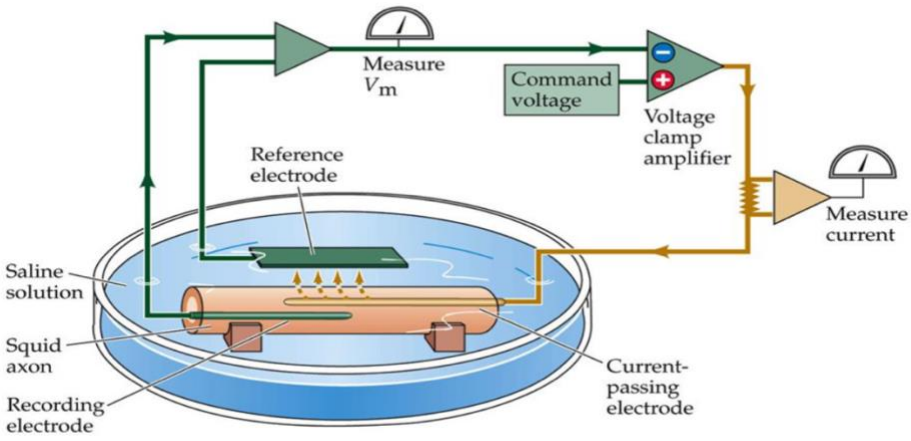

Figure 2.2 Voltage-clamp technique. This device was used to obtain the ion currents on axon membranes. In the voltage-clamp technique, the voltage is held constant, and the function of ions currents can be measured. The reference electrode and recording electrode are inserted along the giant squid axon: the membrane voltage (Vm) is the recorded voltage across the membrane. If Vm is not equal to V command, the other electrode sends currents enough to enable Vm= Vcommand. The whole injected current passes the membrane in the form of ionic current. In the membrane, the potassium conductance activates more slowly than sodium conductance. Therefore when there is a change in membrane potential following electrical current stimulation in this technique, the sodium channel acts first and faster than the potassium channel. Thus, the ionic current of an action potential begins with a fast inward sodium current followed by a slower outward potassium current. This current is measured to analyze the nonlinear conducting behavior of the membrane.

The Hodgkin-Huxley equations are about the current-voltage relationship for the squid axon membrane.

we have:

$$V = V_i - V_e - V_{rest}$$

V_i is the intercellular potential.

V_e is the external potential.

V_{rest} is the resting voltage of the cell.

The V_{rest} is considered as -70(mV) for the squid axon

According to Figure 2.1, the (I_m) is equal to the sum of the membrane capacitive current $\left(C\frac{dV}{dt}\right)$ and ionic currents (I_{ionic}). Therefore we consider (I_m) as the injected current (I_{inj}). We will have: $I_{inj} = I_{ionic} + C\frac{dV}{dt}$ → from this equation, we get the following formula of: $\frac{dV}{dt} = \frac{-i_{ionic}+i_{st}}{c}$

We also know, $I_{ionic} = i_{Na} + i_k + i_L$, therefore we have:

$$I_m = C_m\frac{\partial V}{\partial t} + G_{Na}(V_m - V_{Na}) + G_k(V_m - V_k) + G_L(V_m - V_L)$$

By substituting $\frac{dV}{dt}$, we have the following main formula for membrane voltage changing by time (V'):

$$V' = \frac{-g_{Na}m^3h(V - V_{Na}) - g_k n^4(V - V_k) - g_L(V - V_L) + i_{st}}{c}$$

Together with

$$m' = [-(\alpha_m + \beta_m) \cdot m + \alpha_m] \cdot k$$

$$n' = [-(\alpha_n + \beta_n) \cdot n + \alpha_n] \cdot k$$

$$h' = [-(\alpha_h + \beta_n) \cdot h + a_h] \cdot k$$

To calculate independently of geometric parameters, we determine the currents that pass through the membrane 1cm^2. Therefore, all currents become current densities, and c will be per cm^2.

$$i_{st} = \frac{I_{inj}}{2\pi r l}$$

i_{st} is the stimulation current.

I_{inj} is the injecting current.

l is the length of the axon.

Explanation of temperature factor k:

T (in Celsius) is considered as $k = 3^{0.1T-0.63}$ (with coefficient k for temperature).

α and β based on experimental are:

$$\alpha_m = \frac{2.5-0.1V}{e^{2.5-0.1V}-1} \quad \text{and} \quad \beta_m = 4 \cdot \mathrm{e}^{-\frac{V}{18}}$$

$$\alpha_n = \frac{1-0.1V}{10.(e^{1}-0.1V-1)} \quad \text{and} \quad \beta_n = 0.125 \cdot e^{\frac{-V}{80}}$$

$\alpha_h = 0.07 \cdot e^{-\frac{V}{20}}$ and $\beta_h = \frac{1}{e^{3-0.1V}+1}$

V(0)=0, m(0)=0.05, n(0)=0.32, h(0)=0.06

The Hodgkin-Huxley model was determined with the experimental set-up temperature with T = 6.3 ° C (k = 1) (Rattay 1990).

2.2.2 The Frankenhaeyser-Huxley model

Later in 1964, Frankenhaeuser and Huxley reviewed voltage-clamp data for frog at their nodes of Ranvier of myelinated nerve fiber of the experimental animal.

The Frankenhaeuser-Huxley model contains 5 differential equations and 36 parameters. It describes fiber membrane potential during electrical stimulation. In this model, there is the inactivation of sodium channels (stated by h in the formula), the activation state of the potassium channel (stated by n in the formula), the activation of sodium channels (stated by m in the formula) and, , and also the activation state of a nonspecific ion channel (stated by p in the fomula). These variables for activation and inactivation are the gating kinetics of the different ion channels.

Frankenhaeuser-Huxley equations differ from the Hodgkin-Huxley equations by using permeabilities instead of using the conductance of the ions channels in the nerve fiber membrane. Also, Professor Frank Rattay, in his book of Electrical Nerve Stimulation (Rattay 1990), concluded three differences in the Frankenhaeuser-Huxley model and Hodgkin-Huxley model; which are listed below:

(i) In the Hodgkin-Huxley model, the leakage current is much larger.

(ii) In the threshold region, the model Frankenhauser-Huxley is much more sensitive.

(iii) In the Frankenhaeuser-Huxley model, the afterpotential shows only a minimal hyperpolarization effect. Therefore the voltage does not become negative in the Frankenhaeuser-Huxley model.

The Frankenhaeuser-Huxley model calculations are summarized below:

$$i_{st} = i_{Na} + I_k + i_p + i_L + \mathrm{C} \cdot V'$$

$$V' = \frac{-i_{Na} - I_k - i_p - i_L + ist}{c}$$

$$i_{Na} = P_{Na} m^2 h \frac{EF^2}{RT} \frac{[Na]_o - [Na]_i e^{\frac{EF}{RT}}}{1 - e^{\frac{EF}{RT}}}$$

$$i_k = P_k n^2 \frac{EF^2}{RT} \frac{[K]_0 - [K]_i e^{\frac{EF}{RT}}}{1 - e^{\frac{EF}{RT}}}$$

$$i_p = \mathrm{Ppp}^2 \frac{EF^2}{RT} \frac{[Na]_0 - [Na]_i e^{\frac{EF}{RT}}}{1 - e^{\frac{EF}{R1}}}$$

$$i_L = g_L(V - V_L)$$

Please, check the Glossary for the permeabilities constant values.

Where:

$$m' = -(\alpha_m + \beta_m) \cdot m + \alpha_m$$

$$n' = -(\alpha_n + \beta_n) \cdot n + \alpha_n$$

$$h' = -(\alpha_h + \beta_h) \cdot h + \alpha_h$$

$$p' = -(\alpha_p + \beta_p) \cdot p + \alpha_p$$

α and β by experimental data calculated as:

$$\alpha_m = \frac{0.36 \cdot (V-22)}{1-e^{\frac{22-V}{3}}} \quad \text{and} \quad \beta_m = \frac{0.4 \cdot (13-V)}{1-e^{\frac{V-13}{20}}}$$

$$\alpha_n = \frac{0.02 \cdot (V-35)}{1-e^{\frac{35-V}{10}}} \quad \text{and} \quad \beta_n = \frac{0.05 \cdot (10-V)}{1-e^{\frac{V-10}{10}}}$$

$$\alpha_h = -\frac{0.1 \cdot (V+10)}{1-e^{\frac{V+10}{10}}} \quad \text{and} \quad \beta_h = \frac{4.5}{1+e^{\frac{45-V}{10}}}$$

$$\alpha_p = \frac{0.006 \cdot (V-40)}{1-e^{\frac{40-V}{10}}} \quad \text{and} \quad \beta_p = -\frac{0.09 \cdot (V+25)}{1-e^{\frac{V+25}{20}}}$$

With the initial conditions of:

V(0)=0, m(0)=0.0005 n(0)=0.0268 h(0)=0.8249, p(0)=0.0049

At room temperature, the factor RT / F is about 25mV (Frank Rattay 1990).

The coefficients α and β are multiplied with $Q_{10}^{(T-293)/10}$ for temperatures T (° K). The duration of an action potential is shorter for higher temperatures (especially the duration time of the falling phase of an action potential is less for higher temperatures).

3. Electrical stimulation of the spinal cord (SCS)

3.1 SCS for pain and its clinical usage

The technique of therapeutic electrical stimulation dates from 15AD. A free slave with gout pain walked on an electric torpedo fish incidentally and unexpectedly suffered a grave shock. Afterward, he felt much less gout pain. Eventually, torpedo fish was prescribed to Emperor Claudius for gout and headaches without knowing its mechanism. Later, Galen (131–201 AD) studied electric fish when he realized the electric shock of torpedo fish is the reason for reducing pain and not the torpedo fish itself. This finding marked the start of researching for therapeutic electrical stimulation to cure pain.

A neurosurgeon named Dr. Norman Shealy and his colleagues used SCS for the first time in 1967 to treat chronic and unmanageable cancer pain (Shealy et al. 1967). SCS has been used nowadays to treat combined neuropathic with nociceptive and neuropathic with radicular pain disorders, such as failed back surgical syndrome (FBSS) and complex regional pain syndrome (CRPS). The success rate of 50% pain relief outcomes is about 58% (Taylor et al. 2014). A 20-year study of SCS shows that the efficacy of SCS is 84% for complex regional pain syndromes (CRPS), 82% for postherpetic neuralgia, 77% for ischemic limb pain, 67% for peripheral neuropathy, 62% for FBSS, and 62% for phantom limb pain (Cameron 2004).

SCS implementation involves a two-stage procedure in clinics. First is a trial phase, which lasts for about 3-10 days. During this time, the electrodes array is inserted into the epidural space of the spinal cord (a few levels above the painful spinal segment). It is connected to an external SCS pulse generator. During the trial phase, parameters like amplitude, pulse width, frequency, and other important influencing factors are tested to get maximum pain relief and minimum paresthesia. If the patient achieves more than 50% pain relief, the

patient can proceed to the second stage. In the second stage, the electrode array is applied surgically into the spinal cord and then connected to an impulse generator (IPG). The IPG is placed underneath the skin as well.

Over the past years, there has been a dramatic improvement in SCS. Also, several novel waveform paradigms have emerged in the clinical market. For example, conventional SCS (tonic Stimulation) was the waveform used at the begging clinical use of SCC. Newer approaches with more advantages are explained in the next chapters below.

3.2 Types of stimulation of the spinal cord

3.2.1 Conventional SCS

Conventional SCS (tonic SCS, see Figure 3.1a) involves a moderate frequency between 30-100 Hz applied to the dorsal columns of the spinal cord resulting in the creation of paresthesia (e.g., itching, tingling) over the painful areas (Moffitt et al. 2009). Conventional SCS-induced pain relief occurs between seconds to several hours; however, the SCS-induced paresthesia occurs rapidly (~1 second).

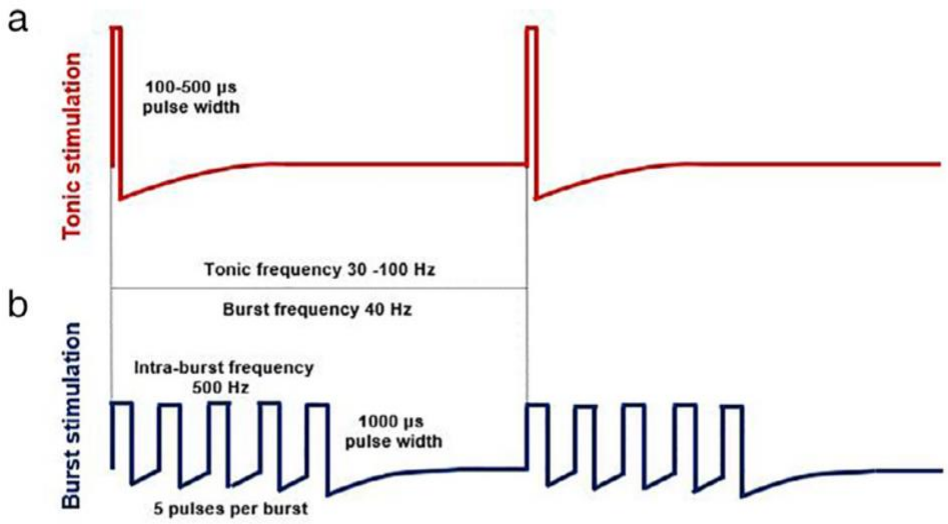

Figure 3,1Toni pattern compared with Burst stimulation pattern.
The tonic stimulation (a) is about 30-100Hz, with the pulse width of 100-500 Micro-Second.
The burst stimulation waveform (b).

3.2.2 Burst SCS

In 2010 De Ridder and colleagues presented the idea of the burst SCS (DeRidder et al. 2010) (see Figure 3.1, Figure 3.2, and Figure 3.3) (Chakravarthy et al. 2018).

In clinical studies, it has been shown the burst- SCS is much more pain relief compared with the tonic stimulation (Deer et al. 2018). The patient's preference for burst SCS is weighted against tonic SCS due to improved pain relief and lack of paresthesia

In several clinical studies, burst SCS, which was applied with sub-sensory amplitude, was more effective for nociceptive back pain component of FBSS and lumbosacral pain (DeRidder and Vanneste 2016a; DeRidder et al. 2013, 2015b, c; Van et al. 2015; DeVos et al. 2014).

Pulse amplitudes used in burst SCS generally are much lower than conventional SCS (Deer et al. 2018 and DeVos et al. 2017). Narrower pulses in SCS require higher amplitudes to activate a nerve. Wide pulse widths, on the other hand, need lower

amplitudes to trigger a nerve. The low amplitudes in burst SCS can partly explain why less somatic sensation of paresthesia in burst SCS is felt (Chakravarthy et al. 2018).

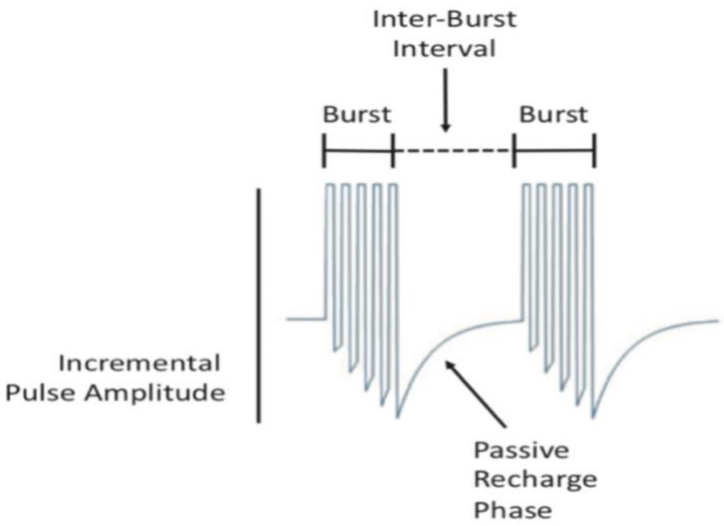

Figure 3.2 Burst stimulation pattern.
Described by DeRidder, burst stimulation delivers five consecutive 500Hz waves at 40Hz burst frequency. Each of the five bursts' pulse width is 1 ms, with incremental pulse amplitude within each of the five consecutive waves.

3.2.3.1 High-frequency SCS

Recently, there has been a systematic shift to high-frequency stimulation, which is paresthesia free. High-frequency SCS usually is about SCS with 1 -10 kHz (HF10 = 10-kHz high-frequency) with low amplitude (1 to 5 mA) pulses which can treat, for example, chronic low back pain with long-lasting effect (Al et al. 2014 and Van Buyten et al. 2013).

3.2.3.2 Comparing HF10 with burst frequency

Kinfe et al. graded 16 FBSS patients with low back pain to perform either HF-SCS or burst SCS for some months. The result was slightly in favor of burst SCS (Kinfe et al. 2016 and Muhammad et al. 2017). In another study (Sajjad et al. 2017), where the pain intensity was measured on a scale of 1-10 from mild pain to worst pain possible, patients with back pain did burst-SCS, and their mean pain decreased from 8±0.76 to 1±1.41. The patients also did 10kHz SCS stimulation, and their mean pain intensity for 10 kHz SCS subjects decreased from 8±0.63 to 3.5±3.27. Figure 3.3 shows three different waveforms of tonic SCS, burst SCS , and High-frequency SCS.

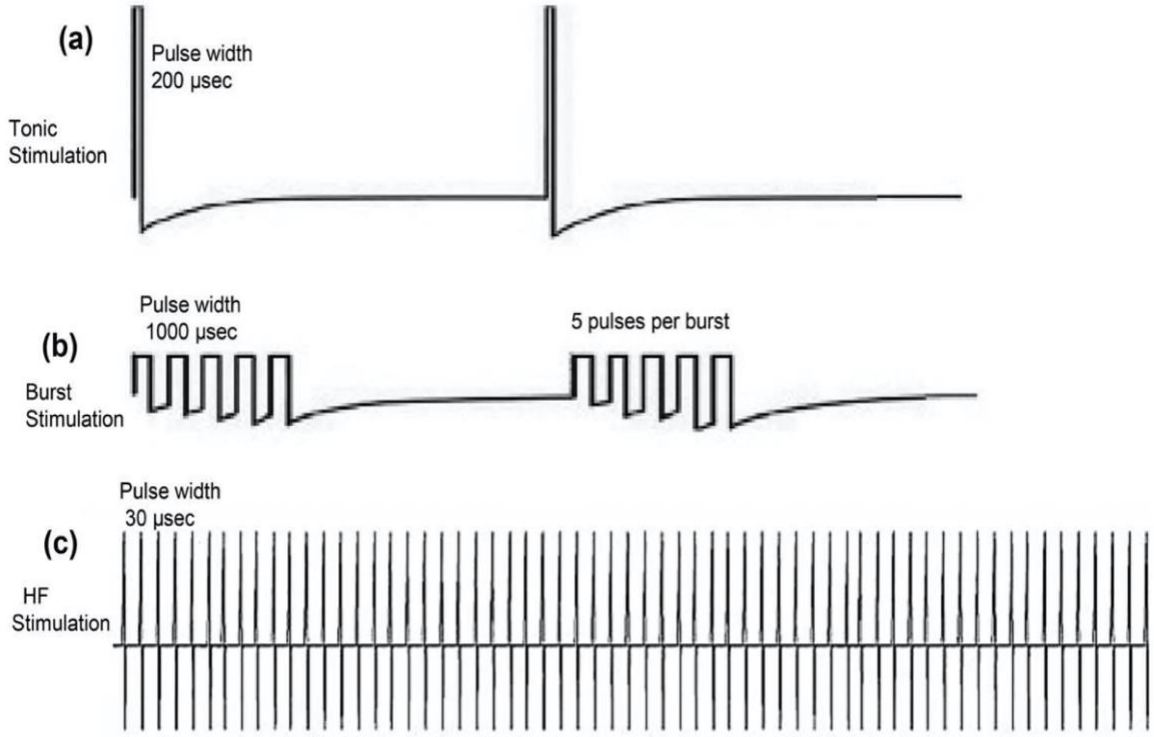

Figure 3.3 Comparing tonic stimulation (a) with burst Stimulation (b) with high-frequency stimulation.

4. Mechanism of action of SCS

4.1 Pain pathway in the spinal cord

During pain, primary afferent fibers (A-Beta, A-delta, and c) transmit a series of action potentials. Theses transmissions go to the dorsal root ganglion and then to the dorsal horn of the spinal cord. In the dorsal horn, the first-order neuron synapse with the second neuron causes the release of substance p. It is important to note that a large number of different neurons are in lamina-1 of the dorsal horn, and 80% of these cells have the neurokinin1 (NK1) receptors for substance p (Todd 2002). The second-order neuron will cross the opposite side of the spinal cord midline. From there, the second-order neuron will ascend to the brainstem and terminate in the thalamus of the brain. The third-order neuron will synapse with the second-order neuron in the thalamus, and help to distinguish the area of injury, and the perception of pain is perceived.

NK1- positive cells in the lamina-1 project to various brain areas such as the thalamus, the periaqueductal grey, and parabrachial area (Todd 2002). These cells also project in the lower part, such as the rostral ventromedial medulla and the region, which has a descending project back to the dorsal horn. Hence, NK1- positive cells in lamina-1 can activate the descending pathways from the brain stem (Mantyh et al. 1997 and Suzuki et al. 2002).

4.2 Gate control theory

In 1965 Ronald Melzack & Patrick Wall first published the gate control theory regarding pain transmission in the dorsal horn of the spinal cord. There is a 'gate' in the dorsal horn where afferent impulses are inhibited or excited. This gate 's control is based on the relative activity of:

- Large-diameter (A-beta) fibers (large fibers activity close the gate).
- Small diameter (A-delta and C) fibers (small diameter fibers activity open the gate).

The large-diameter fibers (non-nociceptive) and small-diameter fibers (nociceptive) in the dorsal horn of the spinal cord are synapsing to the projection neuron (Figure 4.1).

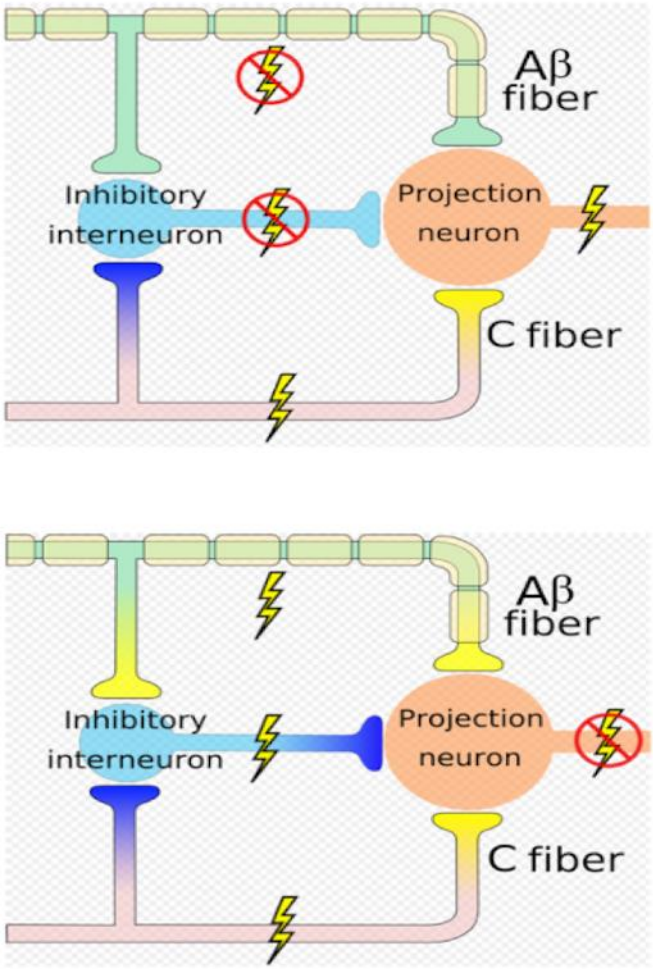

Figure 4.1 The firing of projection neurons determines pain. Excitation of the projection neurons blocked by inhibitory interneurons. The firing of C fibers blocks inhibitory interneurons, thereby resulting in the excitation of projection neurons (as shown in Figure A above). Excitation of the A-beta fibers results in the activation of inhibitory interneuron, resulting in the reduced firing of projection neuron, even if a nociceptor or C fiber is being stimulated (as shown in Figure B) (Jessell et al. 2000).

Conventional SCS, which causes paresthesia, is explained by this theory. The electrical stimulation of myelinated (afferent) A-beta fibers prevents pain transmission from thinly myelinated A-delta fibers and unmyelinated C fibers. Activating A-beta fibers induces paresthesia for the patient (Melzack 1967). Although the mechanism of action in SCS is somehow believed in this theory, it seems it is more complicated than the simple scheme of Figure 4.2.

This theory is the first and best-known theory that described the cause of pain inhibitory modulatory mechanism and can be one of the hypotheses which explain the mechanism of SCS. However, there is a lack of data available to justify the SCS application from the gate control theory perspective. Different biological processes can explain the subcellular mechanism underscoring SCS. The three major biological processes, including neurophysiological, neurochemical, and vascular mechanisms, are elucidated in the following section.

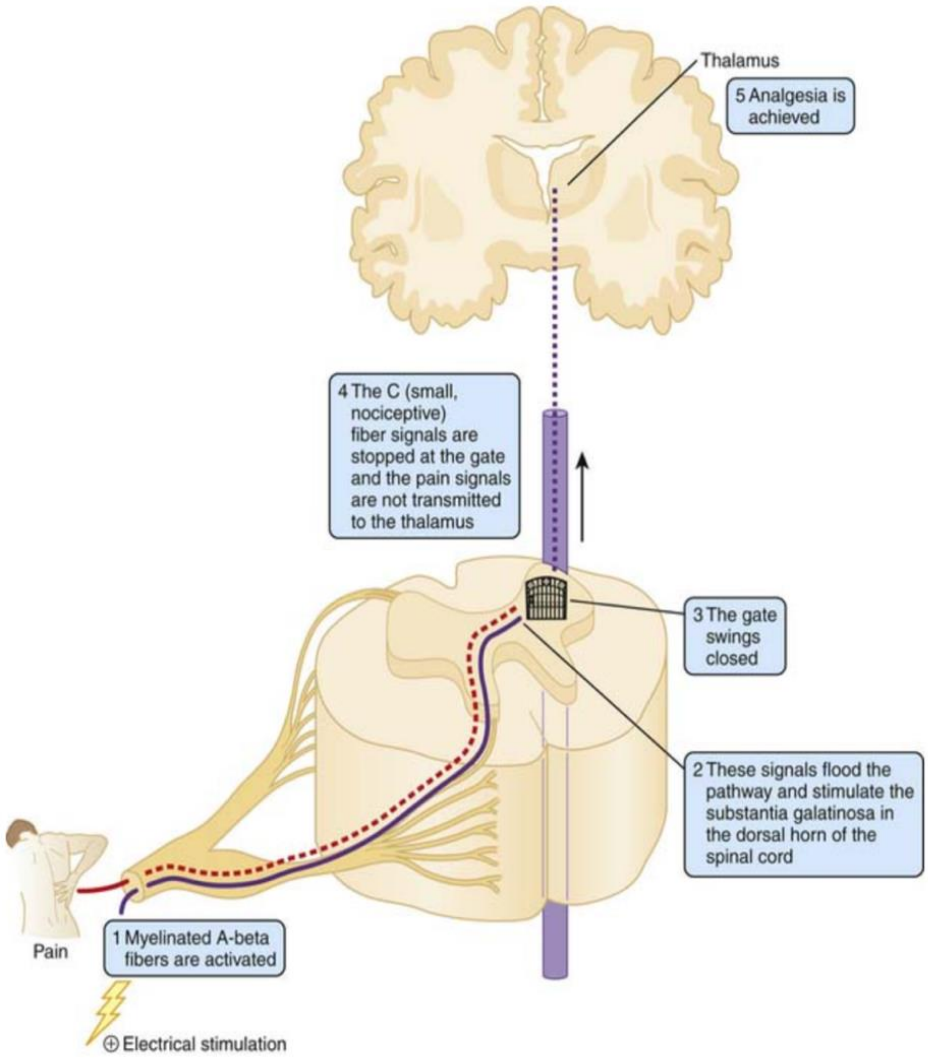

Figure 4.2 A simplistic view of SCS is explained by gate control theory. With the electrical stimulation, Pain signals are blocked at the spinal cord level before transmitting to the thalamus.

4.3 Neurophysiological mechanism

SCS induce an action potential (AP) in a node of Ranvier of a large myelinated axon in the dorsal horn. A generated AP propagates in both directions from the spike initiation site.

Antidromic activation: APs that travel in the opposite direction as the natural nerve fiber direction.

Orthodromic activation: APs that travel in the same direction towards the brain as natural nerve impulses.

The orthodromic impulses traveling to the brain through the A-beta fibers cause paresthesia (Holsheimer 2002; Lee et al. 2011; Hershey et al. 2010). Antidromic impulses, on the other hand, mediates the relief of pain in neuropathic pain.

4.4 Vascular mechanism

The vascular system also plays a significant role in spinal cord stimulation. SCS has been shown to increase blood flow to the spinal segmental cord level's dermatomes, which is stimulated. For example, angina pectoris is a medical term for chest pain caused by the lack of oxygen in the heart muscle. By stimulating the spinal cord, there is re-distribution of coronary blood flow and reduction of myocyte oxygen demand (Deer et al. 2019).

4.5 Neurochemical mechanism

Neuropathic pain has shown hyperexcitability of the wide-dynamic neurons in the dorsal horn of the spinal cord (Yakhnitsa et al. 1997). Single-unit studies show that stimulation of dorsal column inhibits these wide-dynamic neurons. (Hillman et al. 1969; Lindblom and Meyerson 1975; Foreman et al. 1976; Linderoth et al. 2009; Zhang et al. 2014).

Following the SCS application, there is a decrease in the extracellular concentration of glutamate coupled with elevated levels of extracellular GABA concentration (Cui et al. 1997 and Cui et al. 1996). The observed change in the neurotransmitters' activities suppresses hyperexcitable Wide Dynamic Range of neurons, thereby reducing pain (Yakhnitsa et al. 1999).

4.6 High-frequency SCS mechanism

There are several explanations for the high-frequency stimulation. One hypothesis assumes that HF stimulation induces a depolarization blockade (Kilgore and Bhadra 2004 and Kilgore and Bhadra 2014). The HF10 SCS reduces pain without paresthesia. The reason may be the local block of the low-threshold large fibers within the lemniscal path, instead of the generation of traveling impulses (Urasaki et al. 2014, Buonocore and Demartini 2016).

Intriguingly, notable studies have noted the possibility for the selective blockage of C-fibers and A-fibers, based on the frequency input from SCS (Joseph and Butera 2009 and 2011, Joseph et al. 2007). Several studies have shown that alternating high-frequency SCS results in diffusion of the potential action potential in large and small fibers. In a rat study, during the high-frequency SCS using an alternating current of 20kHz and 30 kHz, there was a total block of A-fiber but not the c-fiber (Cuellar et al. 2012). The opposite was also observed in a study using the rat sciatic nerve (Joseph and Butera 2011) in which they

used frequencies above 30 kHz and found that C-fibers but not the A-fibers were blocked. In contrast, the reverse was the case when using lower frequencies between 5–30 kHz.

Another hypothesis assumes that HF stimulation can desynchronize the neuronal clusters that fire in at the same rate. The firing will then become individualized such that each unit is firing at its rate and pattern, thereby diffusing the pain signal and resulting in reduced pain sensation. (Rubinstein et al. 1999 and Litvak et al. 2003).

4.7 Burst SCS mechanism

As we mentioned in chapter 3.2.2, burst stimulation has a more functional and therapeutic advantage than tonic stimulation. A study found that the effectiveness of burst SCS in a rat model with neuropathic pain seems to be linked to the electric charge uses per burst. The study reported that burst stimulation yields more charge per second than tonic SCS to activate various neuronal populations while remaining below the paresthesia threshold (Crosby et al. 2015).

Tang et al. have also revealed that burst stimulation in contrast with tonic stimulation has not impacted gracile nucleus neuronal activity. Low-threshold neurons in gracile nucleus were not inhibited by burst SCS but with tonic SCS their activity was decreased by 20 percent. More specifically, these findings may clarify why patients experience no paresthesia with burst SCS as the gracile nucleus is the tactile sensory target for most of the information coming up from the dorsal columns of the spinal cord (Tang et al. 2014).

5. Other factors for stimulation

5.1 Placement of lead

In general SCS-generated electrical fields are more like a "stage light" forming an "electric field cloth" over the surface of the spinal cord. Fluoroscopic guidance helps to overcome some of the mistakes and difficulties. If the patient experiences paresthesia, it is crucial to correct the leads' positioning to obtain the best efficiency. Stimulation of different body targets requires the lead to insert to a particular stage of spinal cord level (table1- adapted from Deer and Pope 2016).

Spinal level	Target
C2	Face, maxillary region
C2–C4	Neck, shoulder to hand
C4–C7	Forearm to hand
C7–T1	Anterior shoulder
T1–T2	Chest wall
T5–T6	Abdomen
T7–T9	Back and legs
T10–T12	Leg
L1	Pelvis
T12–L1	Foot
L5,S1	Foot, lower limb
S2–S4	Pelvis, rectum
Sacral hiatus	Coccyx

Table 1 Anatomic targets of SCS at specific spinal levels

5.2 Manufactures and companies

In 1980, Medtronic launched the first spinal cord stimulator, approved by the FDA. Advanced neuromodulation systems (ANS), later acquired by St. Jude Medical and Abbott, were another company that used pacemaker technology in the field. In the next few years, Abbott Advanced Bionics, initially owned by Boston Scientific, became another major supplier of the spinal cord stimulator. Nevro company solely produce SCS devices and does not produce any medical devices. Also, the only organization with HF10 SCS is the Nervo SCS. Nevro developed a trial to compare high-frequency 10 kHz therapy with standard SCS for chronic back and leg pain. In May 2015, Nervo received FDA approval of a paresthesia-free product (Kapural et al . 2015)

5.3 Side effect and warning

In total, up to 34 percent of SCS patients could have adverse effects (Turner et al. 2004).

The most common problem in SCS immediately after surgery is lead movement. A silicone adhesive can be used to attach the lead to anchors to reduce lead migration chances in the surgery (Renard and North 2006).

Infection is also a major concern for the patient who is going under implantation operation. Until surgery , patients must check whether they have a body infection. Doctors have to analyze the factors that influence the patient's immune response, particularly cancer or HIV. Smoking weakens a patient's immune system and can prolong healing and increase infection danger. Before the treatment the patient should stop smoking, and the median time of smoking cessation is about six weeks or longer (Møller et al. 2002).

Other adverse effects in SCS include epidural hematoma, dural puncture, spinal cord injury, and so on (Deer et al. 2014)

6. Modeling SCS by MATLAB for single compartment neuron-model

6.1 My MATLAB Simulation results for burst SCS, high-frequency SCS, and tonic SCS on a single-compartment neuron model

In this chapter, the Hodgkin-Huxley mathematical model equations (explained in chapter 2.2) represent the action potential dynamics in a single (non-myelinated) compartment neuron. In this chapter, the Hodgkin-Huxley model is used to do tonic SCS, burst SCS, and HF10 SCS on a single compartment (non-myelinated) mathematical neuron model with the help of MATLAB. MATLAB's computation is performed via a fixed step-size forward or backward Euler process (see appendix A and appendix B).

In this model, the membrane potential of a neuron is introduced by a single variable called V. In the single-compartment model, the membrane potential is the same across the whole neuron.

We were considering the below Hodgkin-Huxley parameters in the MATLAB code for this mission.

% Hodgkin-Huxley parameters in MATLAB:

vRest = -65; % in mV
gNa = 120; % in mS/cm^2
gK = 36; % in mS/cm^2
gL = 0.3; % in mS/cm^2
vNa = 115; % in mV
vK = -12; % in mV
vL = 10.6; % in mV

(See appendix A).

From Figure 2.1 and chapter 2.2, we know the following equations for the squid axon:

$$I_m = C_m \frac{\partial V}{\partial t} + G_{Na}(V_m - V_{Na}) + G_k(V_m - V_k) + G_L(V_m - V_L) \quad \rightarrow$$

$$I_{inj} = I_{ionic} + C\frac{dv}{\mathrm{dt}} \quad \rightarrow$$

$$I_{ionic} = i_{Na} + i_k + i_L \quad \rightarrow$$

$$\frac{dv}{\mathrm{dt}} = \frac{[-i_{ionic} + i_{st}]}{c} \quad \rightarrow$$

$$V' = \frac{-g_{Na}m^3h(V - V_{Na}) - g_k n^4(V - V_k) - g_L(V - V_L) + i_{st}}{c}$$

Where:

$$m' = [-(\alpha_m + \beta_m) \cdot m + \alpha_m] \cdot k$$

$$n' = [-(\alpha_n + \beta_n) \cdot n + \alpha_n] \cdot k$$

$$h' = [-(\alpha_h + \beta_n) \cdot h + a_h] \cdot k$$

M, h, and n represent open probabilities, and their values are always between 0 and 1. The m represents sodium channel activation, and h represents sodium channel inactivation while n represents potassium channel activation.

Consequently, we write the following MATLAB code for the membrane potential with respect to m, h, and n. We used a Backward Euler or Forward Euler approach for computing in MATLAB. Here 'FE' stands for Forward EULER, and 'BE' stands for Backward EULER (see Appendix A).

```
vVec(i+1) = vT + ((-iIon+iStim)/c)*tDt;
switch solver
    case 'FE'
        mVec(i+1) = mT + (alphaM(vT)*(1-mT)- betaM(vT)*mT)*tDt;
        hVec(i+1) = hT + (alphaH(vT)*(1-hT)-betaH(vT)*hT)*tDt;
        nVec(i+1) = nT + (alphaN(vT)*(1-nT)-betaN(vT)*nT)*tDt;
    case 'BE'
        mVec(i+1) = (mT+tDt*alphaM(vT))./(1+tDt*(alphaM(vT)+betaM(vT)));
        hVec(i+1) = (hT+tDt*alphaH(vT))./(1+tDt*(alphaH(vT)+betaH(vT)));
        nVec(i+1) = (nT+tDt*alphaN(vT))./(1+tDt*(alphaN(vT)+betaN(vT)));
  end
vT = vVec(i);
```

```
mT = mVec(i);

hT = hVec(i);

nT = nVec(i);
```

Besides that, I used MATLAB to model (i) tonic SCS waveform, (ii) burst SCS waveform, and (iii) high-frequency SCS waveform. The iStim, which is the stimulus injected current, can be separately replaced by each stimulation waveform type. Therefore, on the single-compartment neuron model created by the MATLAB code, we can see the membrane voltage induced by each of the three SCS waveforms types.

6.1.1. Conventional (tonic) SCS MATLAB model results:

Chapter 3.2.1 refers to the traditional (tonic) SCS scheme. Here I used the aid of MATLAB to model the tonic SCS waveform. Then I used this waveform to activate the single compartment neuron model of Hodgkin-Huxley (substituted tonic SCS waveform result to iStim). See Appendix B (Figure6.1).

Please note, all patients experience different degrees of perception and pain. The tonic SCS amplitude level should be programmed high enough to mask patient discomfort.

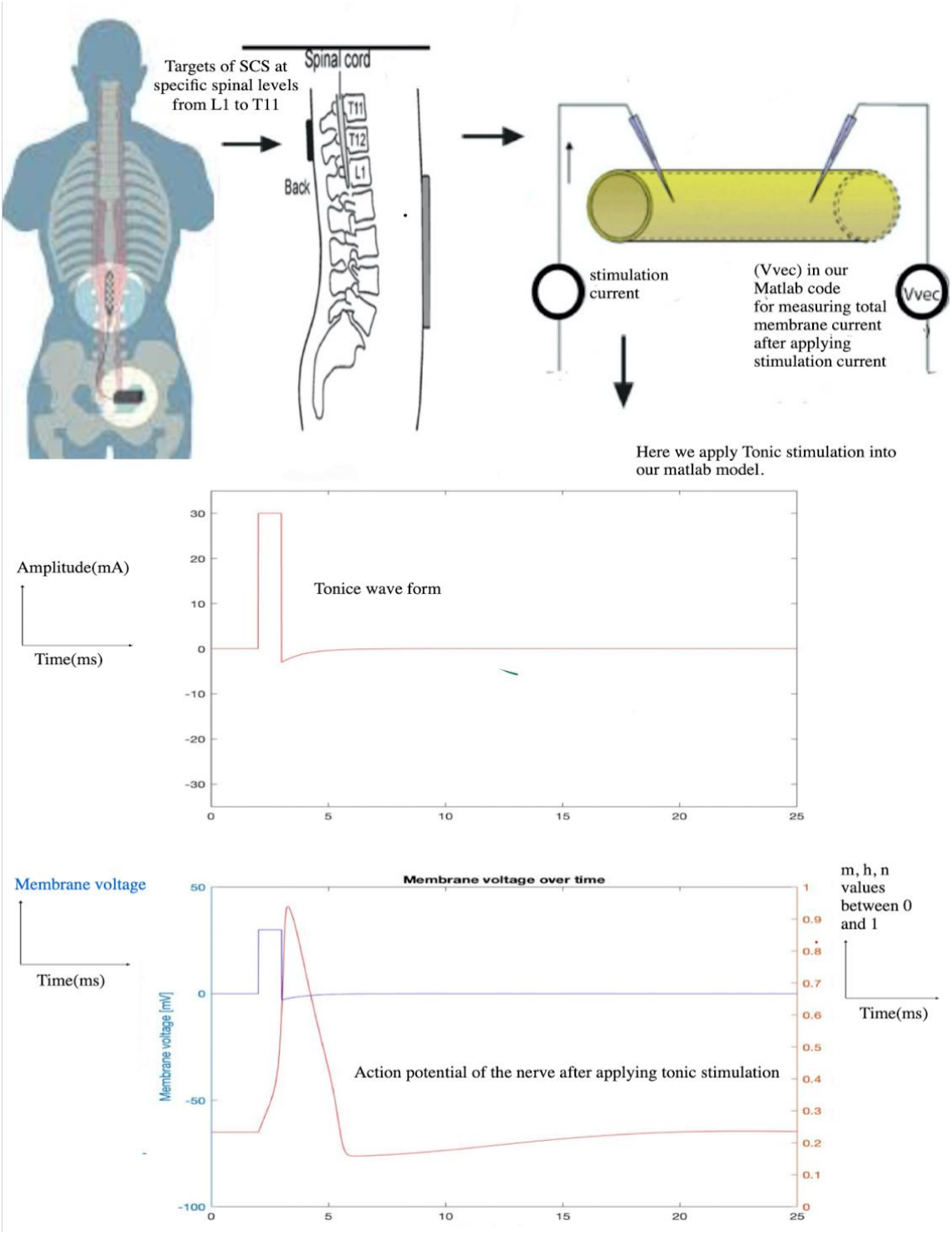

Figure 6.1 The action potential is illustrated for the following tonic stimulation.
As one can see from the illustration, with the stimulation of tonic SCS, the neuron reached the threshold for an action potential.

Please note, for this neuron's second action potential, if we apply the second SCS impulse during the absolute refractory time (no matter how intense the stimulus is), the neuron cannot produce another action potential in this period. Only during or after the relative refractory period the neuron can be stimulated again. The neuron should be stimulated with a greater stimulation during the relative refractory period to get the neuron to reach the next action potential threshold. The next tonic impulse SCS, therefore, should be after the relative refractory period, time cycle, to stimulate the neuron with the same tonic SCS waveform.

6.1.2. Burst SCS MATLAB model results

Chapter 3.2.2 refers to the burst SCS definition. The MATLAB simulation for Burst SCS is shown in Figure 6.2.

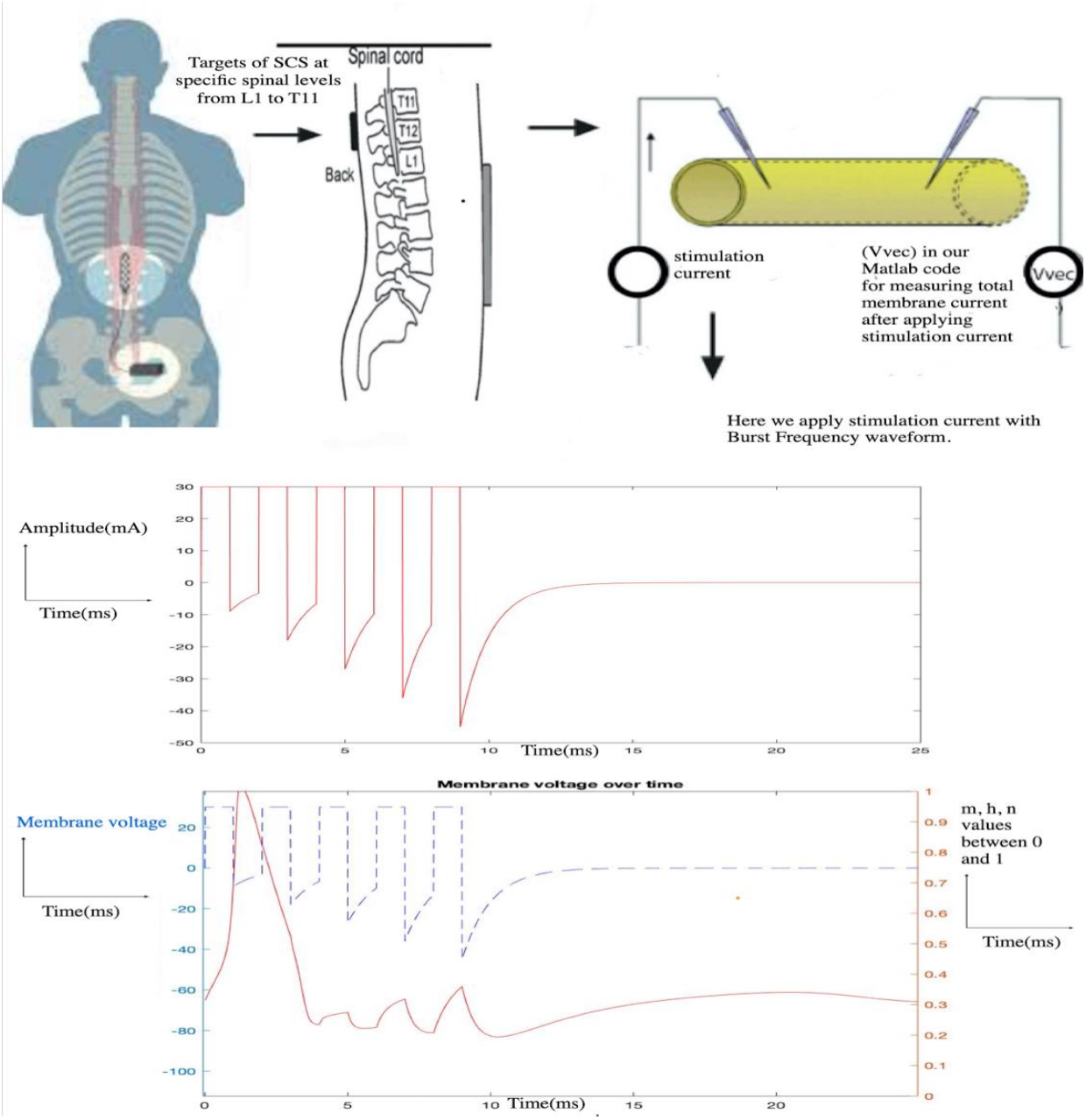

Figure 6.1 The action potential changes after applying the burst stimulation. Each burst SCS waveform delivers five consecutive pulses. In this model, during these five consecutive pulses, the nerve threshold is initially reached, and there is an action potential. Still, the stimulation intensity is not high enough to reach the threshold for a second action potential during the second burst pulse. Therefore, we see the small peaks after the action potential, which is not high enough to become an action potential. Note, however, that axons that are closer to the stimulating electrode may respond with two action potentials, and axons that are in far distance may reach the threshold not by the first pulse but by one of the following ones. This way, the action potentials in a group of stimulated axons will generate non-synchronized firing, which is advantageous for the patient as this method avoids paresthesia.

6.1.3. High-frequency SCS MATLAB model results

High frequency (HF10) SCS has been shown to block the action of potential conduction in the neurons. In this model, we see no action potential is evoked after applying a high-frequency stimulus (inserting high-frequency SCS waveform for the iStim). The sodium and potassium currents are persistently deactivated (m=0 and n=0), thereby preventing the evoking of an action potential (see Figure 6.3).

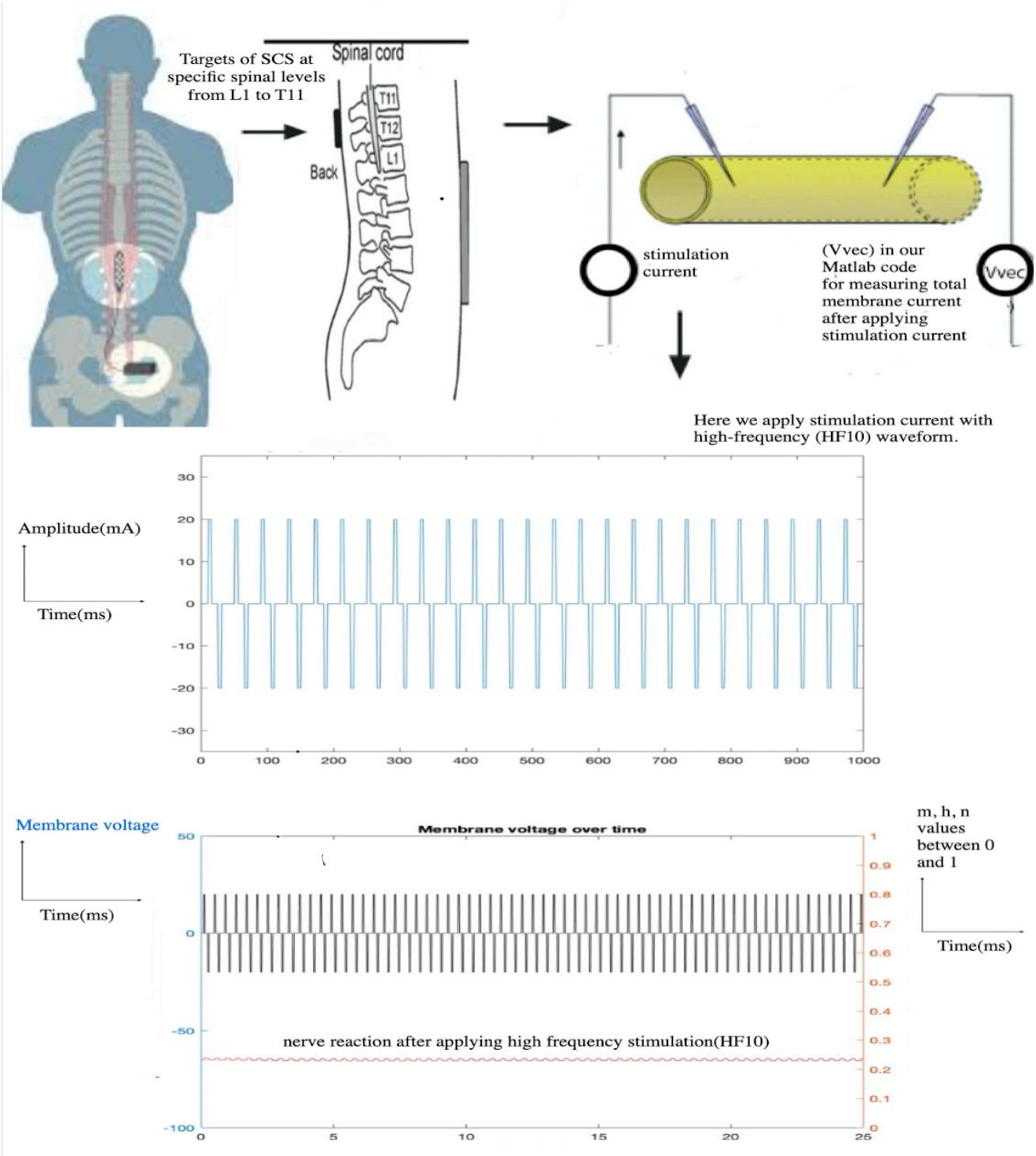

Figure 6.2 There is no evoking potential activity after the high-frequency stimulation is applied. The neuron membrane potential is a flat line at approximately -65 (same as resting state ,vRest defined) after applying high-frequency SCS (Check appendix A, % Hodgkin-Huxley parameters in MATLAB: the vRest = -65; % in mV).

7. SCS conducted by human spinal cord anatomy

7.1 Introduction

The squid axon model used in Hodgkin Huxley has dramatically different characteristics to the human axons. Based on Hodgkin and Huxley's principles and methods, axon models for the simulation of mammalian myelinated axons were later proposed (example, CRRSS model explained in Frank Rattay's book). These computational models must supply accurate information to predict the neural reaction to the SCS correctly. Various simplifications can impact these neural reaction predictions to model design. Having a comprehensive anatomy of the spinal cord is a critical problem for an excellent computational model. See Chapter 7.2 for a brief reference to the anatomy of the spinal cord.

7.2 A brief introduction to spinal cord anatomy:

The spinal cord is an extended form of the brain stem (continuing from the oblong medulla brainstem) and terminating at the vertebral level of L1-L2. In the dorsal and ventral roots, there are 8 cervical nerves, 12 thoracic nerves, 5 lumbar nerves, 5 sacral nerves, and 1 coccygeal nerve (see Figure 7.1). The ventral (front) root carries the motor impulses, and the root dorsal (back) carries the sensory impulses (see Figure 7.2).

The spinal cord is composed of gray matter and white matter. In spinal cord gray matter, there are many cell bodies and a few myelinated axons, but in white matter, there are very

few cell bodies, and it mostly consists of a long-range myelinated axon. The white matter is white due to the whiteness of the fatty substance (myelin) surrounding the nerve fibers (see Figure 7.3).

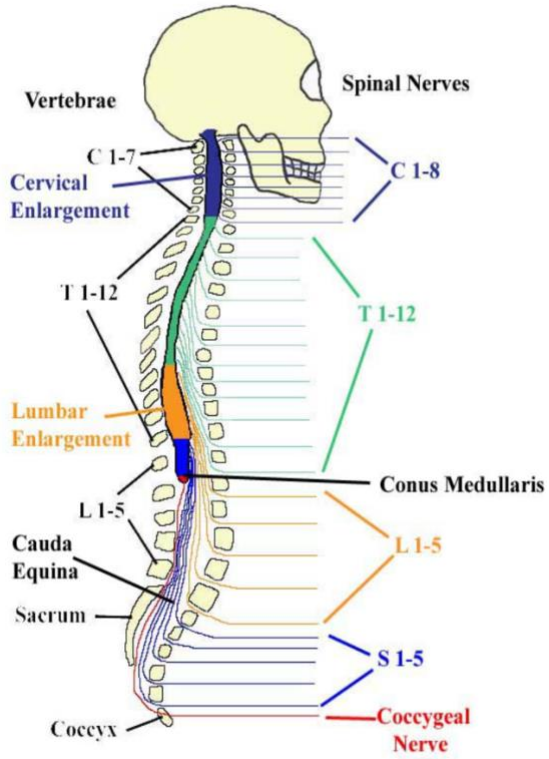

Figure 7.1 Vertebral segments and their spinal nerves at each side of the vertebral column.

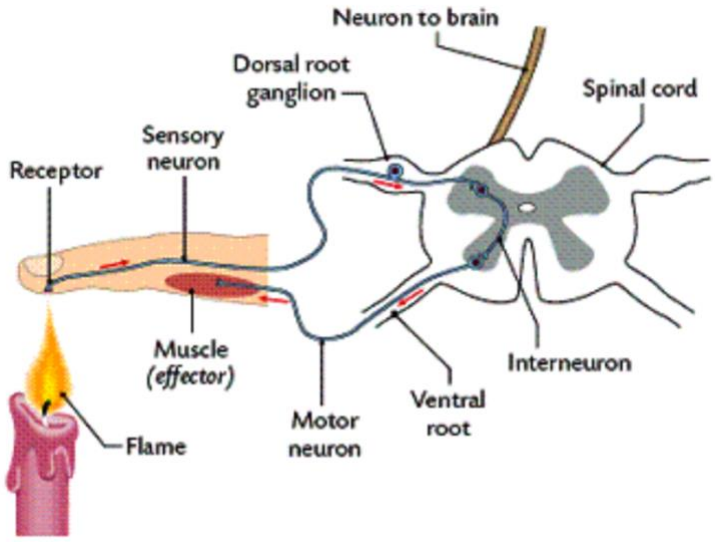

Figure 7.2 The afferent (sensory) and efferent (motor) pathway in the spinal cord.

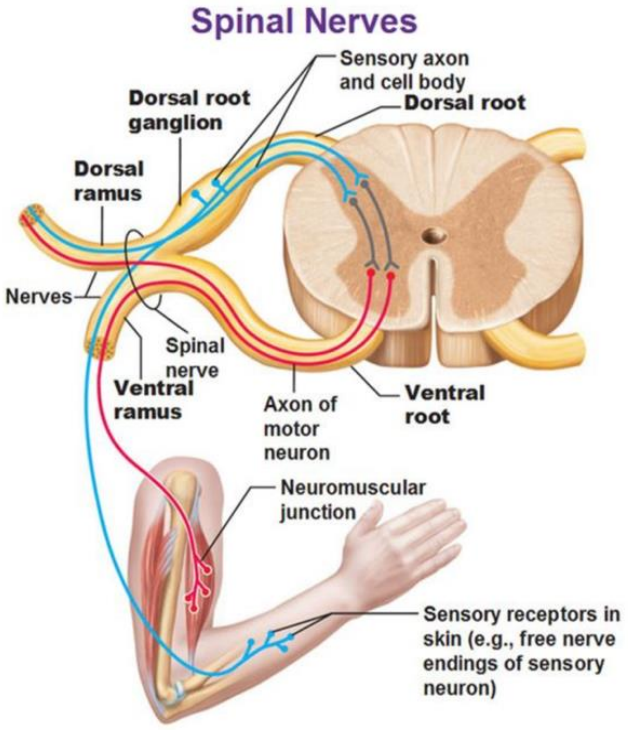

Figure 7.3 It's central H-shaped is the grey matter, and the peripheral is the white matter of the spinal cord.

7.3. Placement of the lead

There have been technical advances in the implementation of SCS over the past 20 years, and a new lead for SCS was introduced. Some examples of lead types are shown in Figure 7.4 and Figure 7.5. Stimulation is provided either by electrodes, which are percutaneously inserted in the epidural space, or by a surgical paddle lead that goes through a laminotomy (Deet et all 2014).

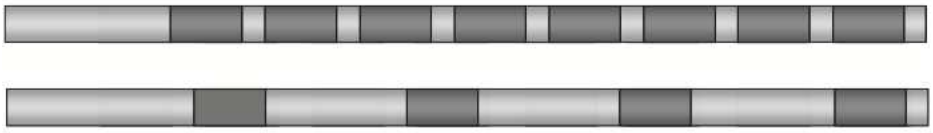

Figure 7.1 Percutaneous leads.

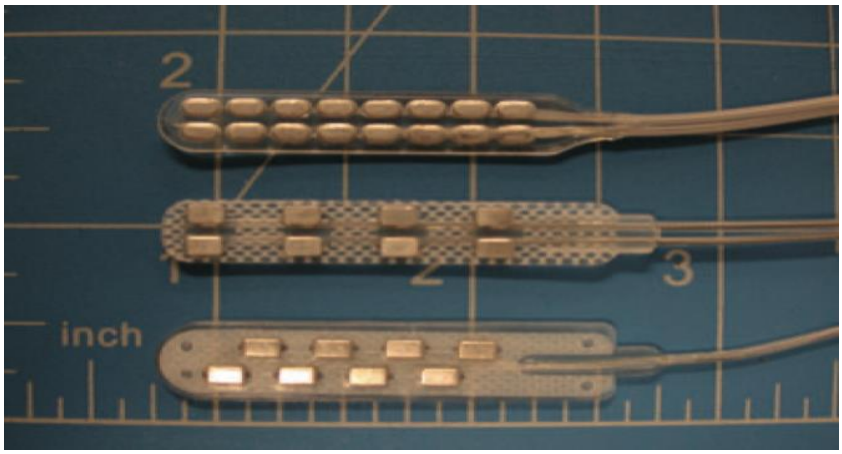

Figure 7.2 Two-column paddle leads.

The surface electrodes of the lead display an ionic current during a stimulation pulse. The ionic current passes through the anatomical structures of the spinal cord from the anode to the cathode. The electric field generated depends on the anodes and cathodes configuration.

Typically, the patient lies in a prone position, and fluoroscopic monitoring is carried out. The lead inserts into the body of the patient until the required vertebral position is reached. The target of lead positioning for SCS is dorsal to dura in the posterior epidural space (see Figure 7.6). The perfect lead position for different patients is different. For example, Figure 7.7 shows the exact midline based on fluoroscopic pictures did not give a patient enough therapeutic outcome, but a physiological midline which could achieve a more painful coverage is achieved by repositioning the lead from the anatomical midline position. This definition implies that the location of dorsal column fiber is variable even from the anatomical midline performed by MRI or CT before the surgery.

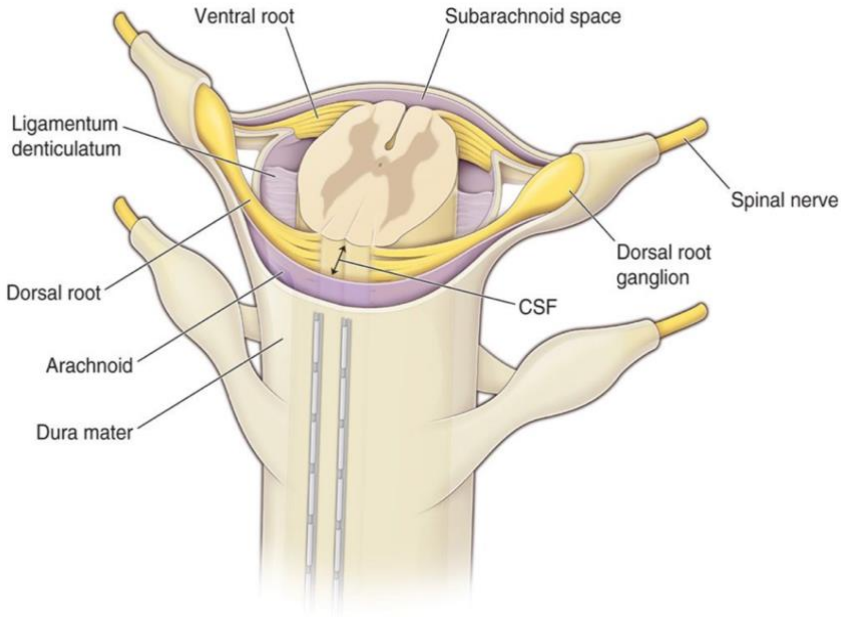

Figure 7.3 Percutaneous leads position in the dorsal to the dura of the epidural space. The thickness of the dorsal cerebrospinal fluid in the spinal canal is the principal determinant of current diffusion.

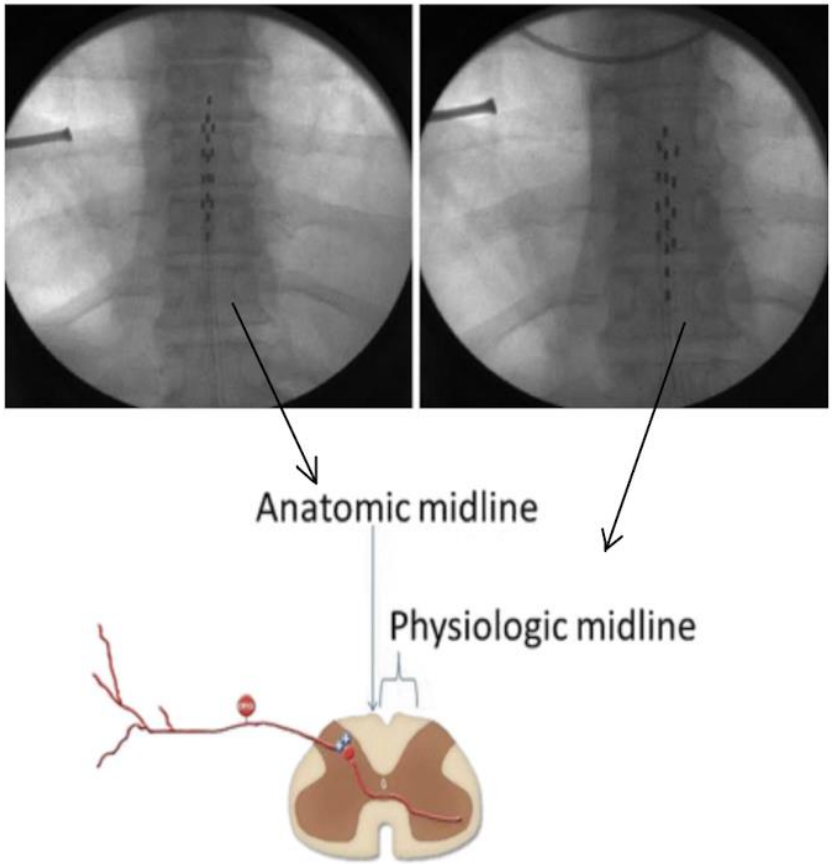

Figure 7.4 Anatomical midline vs. Physiological Midline.
Fluoroscopic image obtained from the anatomical midline during first placement (left photo). In the right picture, a fluoroscopic image is obtained from the physiological midline, which is achieved after relocating leads to have more pain coverage.

7.4. Fiber location in the spinal cord and SCS

The definition of the location of different fibers in the spinal cord is a bit practical, but it is as critical as the lead's location. The fibers' location within the spinal cord is variable, but certain general concepts may also be discovered. The dorsal column's fibers are arranged somatotopically (Figure 7.8).

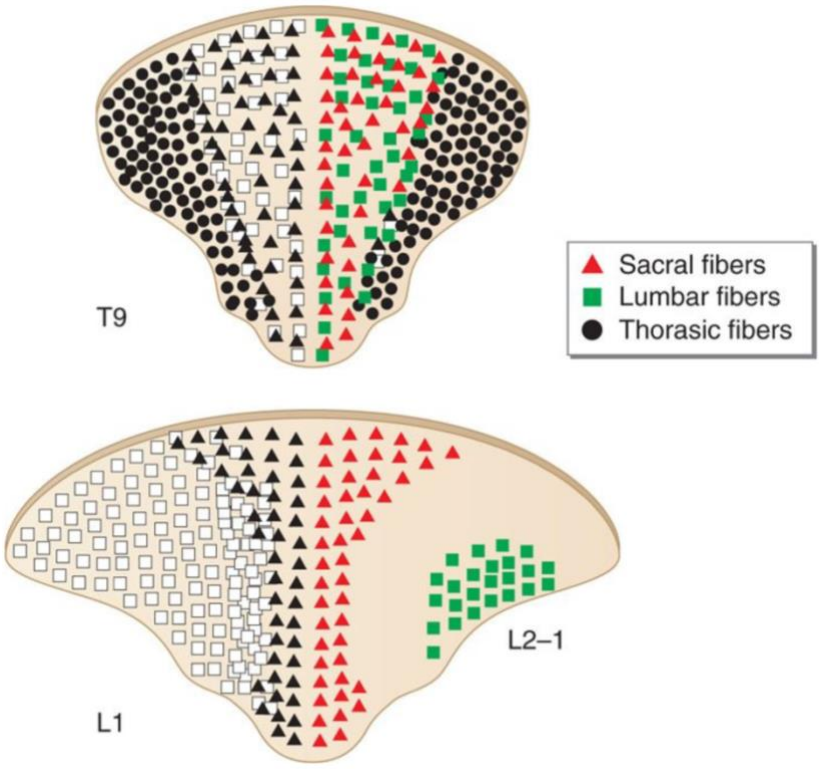

Figure 7.5 The structure of the dorsal column fibers. T9 is in this image for the ninth thoracic vertebra segment, and L1 stands for the first lumbar spinal segment and root.

Previous reports of recruiting particular fiber types during SCS was limited to virtual computer models simulation. (Holsheimer et al. 2002) concluded in dorsal epidural space, myelinated nerve fibers are more likely to be selectively stimulated by SCS than small fiber diameters as they are larger in diameter. However, the fiber distance to the SCS lead

is another significant factor, and the dorsal column fibers closer to the lead are more sensitive than the distance fibers (Rattay et al. 2014).

8. Reference

Al-Kaisy A, Van Buyten JP, Smet I, Palmisani S, Pang D, Smith T. Sustained effectiveness of 10kHz high-frequency spinal cord stimulation for patients with chronic, low back pain: 24-month results of a prospective multicenter study. Pain, Med. 2014; 15:347–54.

Beck PW, Handwerker HO. Bradykinin and serotonin effects on various types of cutaneous nerve fibers. 1974.

Berberich P, Hoheisel U, Mense S. Effects of a carrageenan-induced myositis on the discharge properties of group III and IV muscle receptors in the cat. J Neurophysiology. 1988; 59(5):1395-1409.

Bonica JJ. Bonica's management of pain. Philadelphia: Lippincott Williams & Wilkins; 2010.

Brownstein MJ. A brief history of opiates, opioid peptides, and opioid receptors. Proc Natl Acad Sci. 1993; 90:5391–3.

Bullock TD, Hopkins CD, Popper AN, Rechard R Fray. Electroreception book. Springer Science, Business Media; 2005.

Buonocore M, Demartini L. Inhibition of Somatosensory Evoked Potentials During Different Modalities of Spinal Cord Stimulation: A Case Report. Neuromodulation. 2016; 19(8):882–884.

Cameron T. Safety and efficacy of spinal cord stimulation for the treatment of chronic pain: a 20-year literature review. J Neurosurg. 2004; 100:254-67.

Castro-Junior C, Ferreira L, Delgado M, Silva J, Santos D. Role of Calcium Permeable Channels in Pain Processing. Ion Channels in Health and Sickness. 2018; Oct. 10:107.

Chakravarthy K, Kent AR, Raza A, Xing F, Kinfe TM. Burst spinal cord stimulation: Review of preclinical studies and comments on clinical outcomes, Neuromodulation. 2018; 21(5):431-9.

Cohen SP, Mao J. Neuropathic pain: mechanisms and their clinical implications. BMJ. 2014; 348: f7656.

Colloca L, Ludman T, Bouhassira D, Baron R, Dickenson AH, Yarnitsky D, Freeman R, Truini A, Attal N, Finnerup NB, Eccleston C. Neuropathic pain. Nature reviews Disease primers. 2017;16;3(1):1-9.

Crosby ND, Goodman Keiser MD, Smith JR, Zeeman ME, Winkelstein BA. Stimulation parameters define the effectiveness of burst spinal cord stimulation in a rat model of neuropathic pain. Neuromodulation. 2015; 18:1–8.

Cuellar JM, Alataris K, Walker A, Yeomans DC, Antognini JF. Effect of high-Frequency Alternating Current on Spinal Afferent Nociceptive Transmission. Neuromodulation. 2013; 16: 318–327.

Cui JG, Linderoth B, Meyerson BA. Effects of spinal cord stimulation on touch-evoked allodynia involve GABAergic mechanisms. An experimental study in the mono neuropathic rat, pain. 1996;66: 287–295.

Cui JG, O'Connor WT, Ungerstedt U, Linderoth B, Meyerson BA. Spinal cord stimulation attenuates augmented dorsal horn release of excitatory amino acids in mononeuropathy via a GABAergic mechanism, pain. 1997; 73:87–95.

Danner SM ,Wenger C, Rattay F. Electrical stimulation of myelinated axons. Saarbrücken. 2011.

Davis SF, Kaye AD, editors. Principles of neurophysiological assessment, mapping, and monitoring. Springer. 2020.

DeVos CC, Bom MJ, Vanneste S, Lenders MW, de Ridder D. Burst spinal cord stimulation evaluated in patients with failed back surgery syndrome and painful diabetic neuropathy. Neuromodulation. 2014;17 (2):152-9.

Deer T, Pope J. Disease indications. Atlas of implantable therapies for a pain management book. Springer. 2016; 11–4.

Deer T, Slavin KV, Amirdelfan K, North RB, Burton AW, Yearwood TL, Tavel E, Staats P, Falowski S, Pope J, Justiz R. Success using neuromodulation with burst (SUNBURST)

study: results from a prospective, randomized controlled trial using a novel burst waveform. Neuromodulation: Technology at the Neural Interface. 2018; 21(1):56-66.

Deer TR, Mekhail N, Provenzano D, Pope J, Krames E, Thomson S, Raso L, Burton A, DeAndres J, Buchser E, Buvanendran A. The appropriate use of neurostimulation: avoidance and treatment of complications of neurostimulation therapies for the treatment of chronic pain. Neuromodulation. 2014; 17:571-98.

Deer TR, Pope JE, Lamer TJ, Provenzano D, editors. Deer's Treatment of Pain: An Illustrated Guide for Practitioners. Springer. 2019.

DeRidder D, Plazier M, Kamerling N, Menovsky T, Vanneste S. Burst spinal cord stimulation for limb and back pain. World Neurosurg. 2013; 80(5): 642–649.

DeRidder D, Vancamp T, Lenders MW, De Vos CC, Vanneste S. Is preoperative pain duration important in spinal cord stimulation? A comparison between tonic and burst stimulation, Neuromodulation. 2015;18(1):13–17.

DeRidder D, Vanneste S, Plazier M, Vancamp T. Mimicking the brain: evaluation of St Jude Medical's prodigy chronic pain system with burst technology. Expert Rev. Med. Devices. 2015c; 12, 143–150.

DeRidder D, Vanneste S. Burst and tonic spinal cord stimulation: different and common brain mechanisms. neuromodulation. 2016a; 19, 47–59.

DeVos CC, Bom MJ, Vanneste S, Lenders MW, De RD. Burst spinal cord stimulation evaluated in patients with failed back surgery syndrome and painful diabetic neuropathy. Neuromodulation, 2014; 17, 152–159.

Edmeads J. The physiology of pain: a review. Prog Neuropsychopharmacology Biol, Psychiatry. 1983;7(4-6):413-419.

Elliott KJ. Taxonomy and mechanisms of neuropathic pain. seminars in Neurology by Thieme Medical Publishers. 1994; 14:03:195-205

Fairley P. The conquest of pain book. Michael Joseph; 1978.

Feierabend HKP, Choufoer H, Ploeger S, Holsheimer J, van Gool JD. Morphometry of human superficial dorsal and dorsolateral column fibres: significance to spinal cord stimulation. Brain. 2002;125:1137–49.

Foreman R, Beall J, Coulter J, Willis W. Effects of dorsal column stimulation on primate spinothalamic tract neurons. J Neurophysiol. 1976;39(3):534–46.

Grond S, Zech D, Diefenbach C, Radbruch L, Lehmann KA. Assessment of cancer pain. A prospective evaluation in 2266 cancer patients referred to a pain clinic, pain. 1996;107-114.

Hershey B, Valencia CA, Yearwood TL. Pulse width programming in spinal cord stimulation: a clinical study. Pain Physician. 2010; 13:321–35

Hillman P, Wall P. Inhibitory and excitatory factors influencing the receptive fields of lamina 5 spinal cord cells. Exp Brain Res. 1969; 9(4):284–306.

Holsheimer J. Which neuronal elements are activated directly by spinal cord stimulation Neuromodulation. 2002; 5(1):25–31.

Jessell TM, Kandel ER, Schwartz JH. Principles of neural science. 2000.

Joseph L, Butera RJ. Unmyelinated Aplysia nerve sex habitat non-monotonic blocking response to high-frequency stimulation. IEEE Trans Neural Syst Rehabil Eng. 2009; 17:537–544.

Joseph L, Butera RJ. High-frequency. Stimulation selectively blocks different types of fibers in the frog sciatic nerve. IEEE Trans Neural Syst Rehabil Eng. 2011; 19:550–557.

Joseph L, Haeffele BD, Butera RJ. Conduction block induced by high-frequency AC stimulation in unmyelinated nerves. Conf Proc IEEE Eng Med Biol Soc. 2007;1719–1722.

Julius D. TRP channels and pain. Annual review of cell and developmental biology. 2013;29:355-84.

Kapural L, et al. Comparison of 10-kHz high-Frequency and Traditional Low-Frequency Spinal Cord Stimulation for the Treatment of Chronic Back and Leg Pain: 24-Month Results from a Multicenter, Randomized, Controlled Pivotal Trial. Neurosurgery. 2016;79.5:667–77

Kapural L, Yu C, Doust MW, Gliner BE, Vallejo R, Sitzman BT, Amirdelfan K, Morgan DM, Brown LL, Yearwood TL, Bundschu R. Novel 10-kHz high-frequency Therapy (HF10 Therapy) is superior to traditional low-frequency spinal cord stimulation for the treatment of chronic back and leg pain, The SENZA-RCT Randomized Controlled Trial. Anesthesiology. 2015;123: 851–60 FDA approval for HF10 neurons.

Kilgore KL, Bhadra N. Nerve conduction block utilizing high-frequency alternating current. Med Biol Eng, Compute. 2004; 42:394–406.

Kilgore KL, Bhadra N. Reversible nerve conduction block using kilohertz frequency alternating current, Neuromodulation. 2014; 17:242–254.

Kinfe TM, Pintea B, Link C, Roeske S, Güresir E, Güresir Á, Vatter H. High frequency (10 kHz) or burst spinal cord stimulation in failed back surgery syndrome patients with predominant back pain: Preliminary data from a prospective observational study. Neuromodulation. 2016;19(3):268–75.

Koivisto A, Chapman H, Jalava N, Korjamo T, Saarnilehto M, Lindstedt K, Pertovaara A. TRPA 1: A Transducer and Amplifier of Pain and Inflammation. Basic & clinical pharmacology & toxicology. 2014;114(1):50-5.

Laursen WJ, Anderson EO, Hoffstaetter LJ, Bagriantsev SN, Gracheva EO. Species-specific temperature sensitivity of TRPA1. Temperature (Austin). 2015; Feb 11;2(2):214-26.

Lee D, Hershey B, Bradley K, Yearwood T. Predicted effects of pulse width programming in spinal cord stimulation: a mathematical modeling study. Med Biol Eng Comput. 2011;49(7):765.

Lempka SF, McIntyre CC, Kilgore KL, Machado AG. Computational analysis of kilohertz frequency spinal cord stimulation for chronic pain management. Anesthesiology. 2015; 122:1362–1376.

Lindblom U, Meyerson BA. Influence on touch, vibration, and cutaneous pain of dorsal column stimulation in man. Pain. 1975;1(3):257–70.

Linderoth B, Foreman R, Meyerson B. Mechanisms of action of spinal cord stimulation in the textbook of stereotactic and functional neurosurgery, Springer. 2009; 2331–47.

Litvak LM, Smith ZM, Delgutte B, Eddington DK. Desynchronization of electrically evoked auditory-nerve activity by high-frequency pulse trains of a long duration. J Acoust Soc Am. 2003; 114:2066–2078.

Mantyh PW, Rogers SD, Honore P, Allen BJ, Ghilardi JR, Li J, Daughters RS, Lappi DA, Wiley RG, Simone DA. Inhibition of hyperalgesia by ablation of lamina I spinal neurons expressing the substance P receptor. Science. 1997. 10;278(5336):275-9.

Melzack R, Wall PD. Pain mechanisms: a new theory. Survey Anesthesiology. 1967; 11:89–90.

Moffitt MA, Lee DC, Bradley K: Spinal Cord Stimulation: Engineering Approaches to Clinical and Physiological Challenges. In Implantable Neural Prostheses 2, Springer. 2009;155-194.

Møller A, Villebro N, Pedersen T, et al. Effect of preoperative smoking intervention on postoperative complications: a randomized clinical trial, Lancet. 2002; 359:114 –7.

Moore J. A method of preventing or diminishing pain in several operations of surgery. T Cadell. 1784.

Muhammad S, Roeske S, Chaudhry SR, Kinfe TM. Burst or high-frequency (10 kHz) spinal cord stimulation in failed back surgery syndrome patients with predominant back pain: One-year comparative data, Neuromodulation. 2017;20(7):661–7.

Nunemaker CS, Satin LS. A tale of two rhythms: A comparative review of pulsatile endocrine systems regulating insulin and GnRH secretion. Cell Sci Rev. 2005; 2:92–126.

Nunemaker CS, Satin LS. Episodic hormone secretion: A comparison of the basis of pulsatile secretion of insulin and GnRH. Endocrine 2014;47(1):49–63.

Ochoa Jiji, Torebjork HE: Sensation by intramural microsimulation of single mechanoreceptor units innervating the human hand, J physical (lond). 1983; 342:633-654.

Parker JL, Obradovic M, Hesam Shariati N, Gorman RB, Karantonis DM, Single PS, Laird-Wah J, Bickerstaff M, Cousins MJ. Evoked Compound Action Potentials Reveal Spinal Cord Dorsal Column Neuroanatomy, Neuromodulation. 2019; E-pub ahead of print.

Rattay Frank, Simon M Danner, Ursula S. Hofstoetter, and Karen Minassian. Finite Element Modeling for Extracellular Stimulation. 2014;1-12.

Rattay Frank. Analysis of Models for External Stimulation of Axons. IEEE Transactions on Biomedical Engineering. 1986; BME-33(10), 974-977.

Rattay Frank. Electrical nerve stimulation. New York: Springer, 1990

Reilly JP, Freeman VT, Larkin WD. Sensory effects of transient electrical stimulation-evaluation with a neuroelectric model. IEEE Trans Biomed Eng. 1985; 32:1001–1011.

Renard VM, North RB. Prevention of percutaneous electrode migration in spinal cord stimulation by a modification of the standard implantation technique, J Neurosurg Spine. 2006; 4:300–3.

Rovenstine EA, Wertheim HM. Therapeutic nerve block. JAMA. 1941; 117:1599–603.

Rubinstein JT, Wilson BS, Finley CC, Abbas PJ. Pseudospontaneous activity: stochastic independence of auditory nerve fibers with electrical stimulation. Hear Res. 1999; 127:108–118.

Sabatowski R, Schafer D, Kasper SM, Brunsch H, Radbruch L. Pain treatment: A historical overview. Curr Pharm Des. 2004;10(7):701–16.

Sajjad Muhammad, Sandra Roeske, Shafqat Rasul Chaudhry, Thomas Mehari Kinfe. Burst or high-Frequency (10 kHz) Spinal Cord Stimulation in Failed Back Surgery Syndrome Patients with Predominant Back Pain: One Year Comparative Data. 2017; 12611.

Shealy CN, Mortimer JT, Reswick JB. Electrical inhibition of pain by stimulation of the dorsal columns: a preliminary clinical report. Anesth Analg. 1967;46(4):489-91.

Struijk JJ, Holsheimer J, van der Heide GG, Boom HB. Recruitment of dorsal column fibers in spinal cord stimulation: influence of collateral branching. IEEE Trans Biomed Eng.1992; 39:903-912.

Suzuki R, Morcuende S, Webber M, Hunt SP, Dickenson AH. Superficial NK1-expressing neurons control spinal excitability through activation of descending pathways. Nat Neurosci. 2002; 5: 1319 – 26.

Tang R, Martinez M, Goodman-Keiser M, Farber JP, Qin C, Foreman RD. Comparison of Burst and tonic spinal cord stimulation on spinal neural processing in an animal model. Neuromodulation. 2014;17(2):143-151.

Tang R, Martinez M, Goodman-Keiser M, Farber JP, Qin C, Foreman RD. Comparison of Burst and tonic spinal cord stimulation on spinal neural processing in an animal model. Neuromodulation. 2014; 17:143–151.

Taylor RS, Desai MJ, Rigoard P, Taylor RJ: Predictors of pain relief following spinal cord stimulation in chronic back and leg pain and failed back surgery syndrome: a systematic review and meta-regression analysis. Pain Pract. 2014; 14:489-505.

Todd AJ. Anatomy of primary afferents and projection neurons in the rat spinal dorsal horn with particular emphasis on substance P and the neurokinin 1 receptor. Exp Physiol. 2002; 87: 245 – 9.

Torebjark HE, Ochoa JL, Schady W: referred pain from intraneuronal stimulation of muscle fascicles in the median nerve, pain.1984;18:145-156.

Turner JA, Loeser JD, Deyo RA, Sanders SB. Spinal cord stimulation for patients with failed back surgery syndrome or complex regional pain syndrome: a systematic review of effectiveness and complications, pain. 2004; 1:108(1-2):137-47.

Urasaki E, Tsuda M, Nakane S, Toyoda K, Umeno T, Yamakawa Y. Spinal cord stimulation for intractable pain evaluated by a collision study using somatosensory evoked potentials: a preliminary report. Neuromodulation. 2014;17:8:746–752; discussion 752.

Van Buyten JP, Al-Kaisy A, Smet I, Palmisani S, Smith T. High-frequency spinal cord stimulation for the treatment of chronic back pain patients: results of a prospective multicenter European clinical study. Neuromodulation. 2013; 16:59–65 discussion 65–6.

Van Havenbergh T, Vancamp T, Van Looy P, Vanneste S, De Reeder D. Spinal cord stimulation for the treatment of chronic back pain patients: 500-Hz vs. 1000-Hz burst stimulation. Neuromodulation. 2015;18, 9-12.

Van Havenbergh T, Vancamp T, Van Looy P, Vanneste S, De Ridder D. Spinal cord stimulation for the treatment of chronic back pain patients: 500-Hz vs. 1000-Hz burst stimulation. Neuromodulation. 2015;18(1):9-12; discussion.

Yakhnitsa V, Linderoth B, Meyerson BA. Spinal cord stimulation attenuates dorsal horn neuronal hyperexcitability in a rat model of mononeuropathy, pain. 1999; 79:223–233.

Appendix A:

The Hodgkin Huxley neuron-modeling equation in MATLAB:

```
function [] = hh()

clc;

close all;


%% -----------------------------------------------

% HH.m computes the response of a Hodgkin Huxley single-compartment (==local) model

% The computation is done by a fixed step size forward or backward Euler method

%  -----------------------------------------------

%

%   -----------

%   |   1   |

%   -----------

%

%

%% ------------- Step 1: PARAMETERS -------------
```

```
% Solver type
solver = 'BE'; % 'FE'==Forward EULER or 'BE'==Backward EULER

% HH parameters
vRest = -65; % in mV
gNa = 120; % in mS/cm^2
gK = 36; % in mS/cm^2
gL = 0.3; % in mS/cm^2
vNa = 115; % in mV
vK = -12; % in mV
vL = 10.6; % in mV

% Biophysics
c = 1; % in uF/cm^2

% Temporal and stimulus parameters
tStop = 10; % in ms
tDel = 1; % in ms
tDur = 0.5; % in ms
tDt = 0.01; % in ms

I = 30; % in uA/cm^2
```

```
%% ------------ Step 2: COMPUTE ADDITIONAL PARAMETERS ------------

% Compute time step
tSteps = tStop/tDt+1;
timeStep = 0:tDt:tStop;

% Compute initial values
v0 = 0;
m0 = alphaM(v0)/(alphaM(v0)+betaM(v0));
h0 = alphaH(v0)/(alphaH(v0)+betaH(v0));
n0 = alphaN(v0)/(alphaN(v0)+betaN(v0));

% Allocate memory for v, m, h, n
vVec = zeros(tSteps,1);
mVec = zeros(tSteps,1);
hVec = zeros(tSteps,1);
nVec = zeros(tSteps,1);

% Set Initial values
vVec(:,1) = v0;
mVec(:,1) = m0;
hVec(:,1) = h0;
nVec(:,1) = n0;
```

```
%% --------- Step 3: SOLVE ODE ---------
tic
for i=1:tSteps-1

    % Get current states
    vT = vVec(i);
    mT = mVec(i);
    hT = hVec(i);
    nT = nVec(i);

    % Stimulus current
    iStim = 0;
    if i>tDel/tDt && i<(tDel+tDur)/tDt
        iStim = I; % in uA/cm^2
    end

    % Compute change of m, h and n
    switch solver
        case 'FE'
            mVec(i+1) = mT + (alphaM(vT)*(1-mT)-betaM(vT)*mT)*tDt;
            hVec(i+1) = hT + (alphaH(vT)*(1-hT)-betaH(vT)*hT)*tDt;
            nVec(i+1) = nT + (alphaN(vT)*(1-nT)-betaN(vT)*nT)*tDt;
        case 'BE'
            mVec(i+1) = (mT+tDt*alphaM(vT))./(1+tDt*(alphaM(vT)+betaM(vT)));
            hVec(i+1) = (hT+tDt*alphaH(vT))./(1+tDt*(alphaH(vT)+betaH(vT)));
```

```
        nVec(i+1) = (nT+tDt*alphaN(vT))./(1+tDt*(alphaN(vT)+betaN(vT)));
    end

    % Ionic currents
    iNaVec = gNa*mVec(i+1).^3.*hVec(i+1).*(vT-vNa); % in (mS/cm^2)*mV == uA/cm^2
    iKVec = gK*nVec(i+1).^4.*(vT-vK); % in (mS/cm^2)*mV == uA/cm^2
    iLVec = gL*(vT-vL); % in (mS/cm^2)*mV == uA/cm^2
    iIon = iNaVec+iKVec+iLVec;

    % Compute change of v
    vVec(i+1) = vT + ((-iIon+iStim)/c)*tDt; % in ((uA/cm^2)/(uF/cm^2))*ms==mV
end

% adjust to resting voltage
vVec = vVec + vRest;

fprintf('Solve time was %.3f seconds.\n',toc);


%% --------- Step 4: VISUALIZE RESULTS ---------

% Membrane voltage over time
Figure
hold all
```

```
yyaxis left

box on
title('Membrane voltage over time');
plot(timeStep,vVec,'r');
rectangle('Position',[tDel -100 tDur 10],'Edgecolor','r','Facecolor','r');
ylim([-100 50]);
xlabel('Time [ms]')
ylabel('Membrane voltage [mV]')

yyaxis right
plot(timeStep,mVec, 'b')
plot(timeStep,hVec, 'g')
plot(timeStep,mVec.*mVec.*mVec.*hVec, 'm')

%% ------------ DEFINE FUNCTIONS FOR ALPHAS AND BETAS ------------

    function am = alphaM(v)
        am = (2.5-0.1*v)/(exp(2.5-0.1*v)-1);
    end
    function bm = betaM(v)
        bm = 4*exp((-v)/18);
    end
    function ah = alphaH(v)
```

```
        ah = 0.07*exp(-v/20);
    end
    function bh = betaH(v)
        bh = 1/(exp(3-0.1*v)+1);
    end
    function an = alphaN(v)
        an = (1-0.1*v)/(10*(exp(1-0.1*v)-1));
    end
    function bn = betaN(v)
        bn = 0.125*exp(-v/80);
    end
end
```

Appendix B

Tonic Stimulation Waveform defined as input_ii in MATLAB code then use (iStim=input_ii) in the Hodgkin Huxley neuron-modeling equation in MATLAB

```
clc;
close all;
clear;

%%
time_step=0.01;%ms
final_time=1/40*1000;%ms
tStop = 25; % in ms
n=ceil(tStop/final_time);
timeSpan=0:time_step:final_time;timeSpan=timeSpan';%ms
tau=1;%ms
num=1;
den=[1,1/tau];
```

```
Transfer=tf(num,den);
Transfer_d = c2d(Transfer,time_step);
[num_d,den_d]=tfdata(Transfer_d);
den_d=cell2mat(den_d);
num_d=cell2mat(num_d);
input_i=zeros(length(timeSpan),1);
l=0;
input_i(1)=0;
y=ones(1/time_step,1);
i=1;
numbre_of_pulse=1;
Pf=500;%1/s
amplitude=30;
slop=amplitude*0.1;%ms
for k=1:length(input_i)
   input_i(k+1)=-den_d(2)*input_i(k);
%     input_i(k+1)=-amplitude;
   if i<=length(numbre_of_pulse)
      if                    k>(1/Pf*1000)/time_step*numbre_of_pulse(i)                    &&
k<(1/Pf*1000)/time_step*numbre_of_pulse(i)+length(y)
         input_i(k+1)=amplitude;
      elseif k==(1/Pf*1000)/time_step*numbre_of_pulse(i)+length(y)
         input_i(k+1)=-i*slop;
%           input_i(k+1)=0;
         i=i+1;
```

```
        end
    end
end
input_ii=repmat(input_i(1:end-1),n,1);
time_Spann=repmat(timeSpan,n,1);
figure
plot(time_Spann,input_ii,'-r')
ylim([-35 35])
%% -----------------------------------------------
% HH.m computes the response of a Hodgkin Huxley single-compartment (==local)
model
% The computation is done by a fixed step size forward or backward Euler method
%  -----------------------------------------------
%
%   -----------
%   |    1    |
%   -----------
%
%
%% ------------- Step 1: PARAMETERS -------------


% Solver type
solver = 'BE'; % 'FE'==Forward EULER or 'BE'==Backward EULER


% HH parameters
```

```
vRest = -65; % in mV

gNa = 120; % in mS/cm^2

gK = 36; % in mS/cm^2

gL = 0.3; % in mS/cm^2

vNa = 115; % in mV

vK = -12; % in mV

vL = 10.6; % in mV


% Biophysics

c = 1; % in uF/cm^2


% Temporal and stimulus parameters

% tStop = 20; % in ms

tDel = 1; % in ms

tDur = 0.5; % in ms

tDt = 0.01; % in ms

x=30;

I = x;

% I = x.^2; % in uA/cm^2



%% ------------- Step 2: COMPUTE ADDITIONAL PARAMETERS -------------


% Compute time step

tSteps = tStop/tDt+1;
```

```
timeStep = 0:tDt:tStop;

% Compute initial values
v0 = 0;
m0 = alphaM(v0)/(alphaM(v0)+betaM(v0));
h0 = alphaH(v0)/(alphaH(v0)+betaH(v0));
n0 = alphaN(v0)/(alphaN(v0)+betaN(v0));

% Allocate memory for v, m, h, n
vVec = zeros(tSteps,1);
mVec = zeros(tSteps,1);
hVec = zeros(tSteps,1);
nVec = zeros(tSteps,1);

% Set Initial values
vVec(:,1) = v0;
mVec(:,1) = m0;
hVec(:,1) = h0;
nVec(:,1) = n0;
iStim=input_ii;

%% --------- Step 3: SOLVE ODE ---------
tic
for i=1:tSteps-1
```

```
    % Get current states
    vT = vVec(i);
    mT = mVec(i);
    hT = hVec(i);
    nT = nVec(i);

    % Stimulus current
%     iStim = 0;
%     if i>tDel/tDt && i<(tDel+tDur)/tDt
%         iStim = I; % in uA/cm^2
%     end

    % Compute change of m, h and n
    switch solver
        case 'FE'
            mVec(i+1) = mT + (alphaM(vT)*(1-mT)-betaM(vT)*mT)*tDt;
            hVec(i+1) = hT + (alphaH(vT)*(1-hT)-betaH(vT)*hT)*tDt;
            nVec(i+1) = nT + (alphaN(vT)*(1-nT)-betaN(vT)*nT)*tDt;
        case 'BE'
            mVec(i+1) = (mT+tDt*alphaM(vT))./(1+tDt*(alphaM(vT)+betaM(vT)));
            hVec(i+1) = (hT+tDt*alphaH(vT))./(1+tDt*(alphaH(vT)+betaH(vT)));
            nVec(i+1) = (nT+tDt*alphaN(vT))./(1+tDt*(alphaN(vT)+betaN(vT)));
    end

    % Ionic currents
```

```
    iNaVec = gNa*mVec(i+1).^3.*hVec(i+1).*(vT-vNa); % in (mS/cm^2)*mV == uA/cm^2
    iKVec = gK*nVec(i+1).^4.*(vT-vK); % in (mS/cm^2)*mV == uA/cm^2
    iLVec = gL*(vT-vL); % in (mS/cm^2)*mV == uA/cm^2
    iIon = iNaVec+iKVec+iLVec;

    % Compute change of v
    vVec(i+1) = vT + ((-iIon+iStim(i))/c)*tDt; % in ((uA/cm^2)/(uF/cm^2))*ms==mV
end

% adjust to resting voltage
vVec = vVec + vRest;

fprintf('Solve time was %.3f seconds.\n',toc);


%% --------- Step 4: VISUALIZE RESULTS ---------


% Membrane voltage over time
figure
hold all

yyaxis left
```

```
box on
title('Membrane voltage over time');
plot(timeStep,vVec,'r');
plot(timeStep,iStim(1:length(timeStep)),'-b')
% rectangle('Position',[tDel -100 tDur 10],'Edgecolor','r','Facecolor','r');
ylim([-100 50]);
xlabel('Time [ms]')
ylabel('Membrane voltage [mV]')

% yyaxis right
% plot(timeStep,mVec, 'b')
% plot(timeStep,hVec, 'g')
% plot(timeStep,mVec.*mVec.*mVec.*hVec, 'm')
% ylim=([-100 100])

%% ------------- DEFINE FUNCTIONS FOR ALPHAS AND BETAS -------------

function am = alphaM(v)
am = (2.5-0.1*v)/(exp(2.5-0.1*v)-1);
end
function bm = betaM(v)
bm = 4*exp((-v)/18);
end
function ah = alphaH(v)
ah = 0.07*exp(-v/20);
```

```
end

function bh = betaH(v)

bh = 1/(exp(3-0.1*v)+1);

end

function an = alphaN(v)

an = (1-0.1*v)/(10*(exp(1-0.1*v)-1));

end

function bn = betaN(v)

bn = 0.125*exp(-v/80);

end
```